Author

OFOMA, Anthony E.

PG/M.Sc/98/24839

Title

Electrical Resistivity and Magnetic Surveys of Some Parts of Nsukka Local Government Area, Enugu State Nigeria

Faculty

Physical Sciences

Department

Geology

Date

March, 2001

Signature

ELECTRICAL RESISTIVITY AND MAGNETIC SURVEYS OF SOME PARTS OF NSUKKA LOCAL GOVERNMENT AREA, ENUGU STATE NIGERIA.

BY

OFOMA ANTHONY ENEBEKE ***B.Sc. (Hons) GEOLOGY.***

PG/M.Sc./ 98/ 24839.

PROJECT REPORT SUBMITTED TO THE DEPARTMENT OF GEOLOGY IN THE FACULTY OF PHYSICAL SCIENCES IN PARTIAL FULFILMENT OF THE REQUIREMENT FOR THE DEGREE OF MASTER OF SCIENCE (EXPLORATION GEOPHYSICS IN ECONOMIC GEOLOGY).

UNIVERSITY OF NIGERIA, NSUKKA.

MARCH, 2001

CERTIFICATION

MR. OFOMA ANTHONY ENEBEKE, a postgraduate student in the Department of Geology, University of Nigeria, Nsukka has satisfactorily completed the requirement for course and project works for the degree of Master of Science (M.Sc. Exploration geophysics in Economic Geology).

The work embodied in this project report is original and has not been submitted in part or full for any other diploma or degree of this or any other university.

2/7/2001

DR. L.I. Mamah
Supervisor,
Geology Department,
UNN.

2/7/2001

Prof M. C. Ezepue
Supervisor,
Geology Department,
UNN.

2/7/2001

Prof M.C. Ezepue
Head, Department of Geology,
UNN

DEDICATION

This project work is dedicated to all lovers
and proponents of Education within the
OFOMA DYNASTY of Amakwa,
Ozubulu in Ekwusigo L.G.A.
of Anambra State, Nigeria.
And to the memory of my late friend,
NKEMJIKA ARINZE.

ACKNOWLEDGMENT

I wish to express my sincere gratitude to Dr L.I. Mamah and Prof. M .C Ezepue, my supervisors whose criticisms, suggestions and dedication contributed in making this work successful, and to all the lecturers in the Department of Geology UNN.

I am also grateful to my parents Engr. and Mrs. F.M Ofoma (Umeozogalanya), for their encouragement to me to continue with my education despite the odds. To my elder brother, Mr C.C. Ofoma (CJ), for the sponsorship of this programme and to my younger ones Sonma and Enyeobi for their beautiful pieces of advice.

The encouragement and assistance from my colleagues and friends Edwin Yenika, Victor Ukwueze, Amobi Johnson, Ralph Akukwe, Ephraim Affia, Lapei Peters, Vincent Aneto, Uche Nehezor, Ifeyinwa Adibe, Michael Ekweazor, Emeka Okoli and others are gratefully acknowledged. Furthermore, Mr. Ejike Uboaja (the technologist), Azubike Umerah, Chinedu Ozokafor, Onyebuchi Alanze, Anayo Onyezebe, who helped in one way or the other during the period of data acquisition, I say thank you to you all, I am grateful. And to you Ebele Monwuba who typed this work, I say thank you.

Finally, I wish to thank the Almighty God for his mercies, guidance and protection during the period of this programme.

LIST OF FIGURES

LIST OF TABLES

TABLE OF CONTENTS

ABSTRACT

Seven resistivity profiling covering about 4,725m (4.725km) and eleven magnetic profiling covering about 9,760m (9.760km) were carried out within the University of Nigeria, Nsukka and its surrounding areas, the essence was to use resistivity and magnetic methods to determine subsurface characteristics in terms of paleotectonic regime (fault, fracture etc), and attempt a comparison of the ground magnetics with the aeromagnetic map as well as a comparison of the values obtained from the resistivity and magnetic surveys using statistical method.

The areas covered show resistivity high and low as well as minor distortions. High resistivity values are indicative of low conducive materials, e.g. laterite, dry sand etc and low porosity areas. While low resistivity values are suggestive of high conductive materials e.g. shale, clay etc and loose materials. The minor distortions might be suggestive of fault or joint set.

Magnetic highs, lows and minor distortions were equally observed in the study area, as well as changes in polarity from negative to positive and/or changes in polarity from positive to negative, this is suggestive of probably minor fault or fracture point or even joint set or rock discontinuity. The ground magnetic survey did not show enough anomalies.

Cross-section of the aeromagnetic map revealed flat but linearly increasing shape, this suggests presence of magnetically susceptible materials. The geologic map revealed dome shape (refer to Fig. 1a and 1b in the pocket at the last page).

Cross correlation analysis of the apparent resistivities obtained with the magnetic value showed that all the profiles were uncorrelated. Their degrees of freedom, test of significance, and p% were equally determined.

CHAPTER ONE

INTRODUCTION

1.1 LOCATION AND ACCESSIBILITY

The project area is part of Nsukka local Government area in Enugu State. It lies between Latitude 6^0 44′ N and 6^0 55′ N and longitude 7^0 22′ E and 7^0 30′ E. It has a total area of about 163km^2 and shows major towns like Nsukka, Ibegwa, Opi Lejja etc (Fig 1a in the pocket at the last page). The renovated Opi-Nsukka road and the Obollo Afor – Nsukka Road makes it accessible into Nsukka town and the University of Nigeria Nsukka campus. Further, tarred roads extend to other towns like Lejja, Ovoko, Ibegwa etc through Nsukka town; footpaths are also available in this areas for easy accessibility where roads are either inexistent or unmotorable. (see fig. 2 for the location of the study area in the map of Nigeria).

1.2 PHYSIOGRAPHIC EVOLUTION.

The major Physiographic expressions in the region covering the area are the fork – like ridges trending NE – SW from

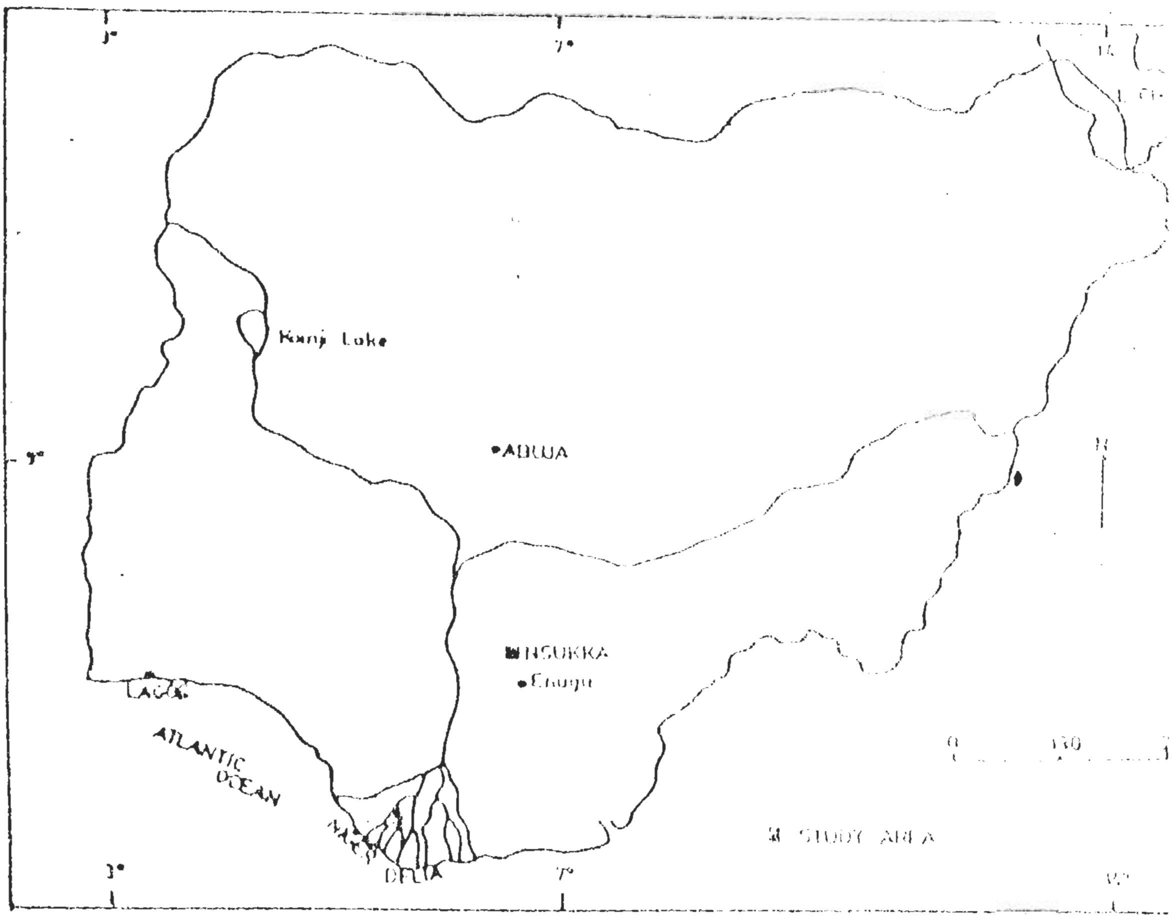

FIG 2. MAP OF NIGERIA SHOWING STUDY AREA

Nsukka towards Lejja area, numerous isolated hill that make the terrain undulating that has resisted intensive denudational activity under high humid condition during the tertiary (Umeji, 1980). Presently the hills consist of intercalations of mudstones and hard lateritic carapace, forming outliers over the older Ajali sandstones.

The topographic setting constitutes part of the major planation surface on North-south trending prominent cuesta in the south-eastern Nigeria. (the Enugu- Okigwe escarpment). The Nsukka plateau surface has an average elevation of 430-460m above sea level. (Umeji, 1980).

1.3 VEGETATION AND CLIMATE.

The study area is part of the rain forest-savana belt (Igbozurike 1975) close and semi-closed forest. Disparity in the vegetation cover exists, in area underlain by sandstones, rolling grass lands. While in the lowly shaly terrains vegetation is dense.

The region also experiences climatic fluctuations (Inyang, 1975). There are usually four months of dry season and eight months of wet season. The wet season starts from March through to October, while the dry season usually span through November to February. This climatic circle is caused by the North – South fluctuation of the zone of discontinuity between the dry continental Sahara air and humid Atlantic air (Ganier in Ozoko, 1988).

1.4 OBJECTIVE OF STUDY.

The aim of the present study is to use resistivity and magnetic methods to study the sub-surface characteristics of some part of Nsukka Formation.

Attempt a comparism of the ground magnetics with the aeromagnetic map with special emphasis at eleven (11) locations within the study area.

Use both geological survey and resistivity method to investigate the presence and extent of paleotectonic regime (fault and joint). The surface resistivity measurements for detection and delineation of faults was employed across all the study area.

Finally, use statistical methods to correlate the two variables, magnetic and resistivity values.

1.5 REVIEW OF PREVIOUS WORK.

The Geological Survey of Nigeria started the mapping of the southeastern Nigeria in 1922. Shell B.P carried out an extensive mapping of the southeastern Nigeria between

1938-1957. The cuesta topography of the study area was first recognised by Groove (1951) but he thought the existing relief was a sub-aerial denudation surface, Quaternary climatic change was suggested by Ofomata (1974), while Umeji,(1980) believed it was a sporadic uplift separated by a period of erosion lateritization that carved the topographic expression. Three major tectonic and depositional cycles was recognised in the south eastern Nigeria (short and stable, 1967; Murat, 1970; Burke et al, 1970).

The Geological investigation of the study area have been carried out by simpson(1954), Reyment (1965), Hoque and Ezepue (1977) and Banerjee (1979). Tattan (1944) and simpson (1954) named the three geologic formation that outcrop in the area as upper coal measures, the false Bedded sandstone and the lower coal measures. These were appropriately renamed as Nsukka Formation, Ajali sandstone and the Mamu Formation respectively by Reyment (1965), Reyment proposed the ammonite zonational scheme for the Southeastern Nigeria, subsequent workers (Wozdu and Kogbe, 1982; Zaborski, 1983; Popoff et al, 1986) also dated Cretaceous sediments using biostratigraphy. Hoque and Ezepue, (1977) described the petrology and paleogeography of Ajali sandstone while Nwajide and Hoque (1982) reported the textural properties of Ajali sandstone as composed of medium- coarse grain sandstone, sub-angular to sub-rounded quartz arenites. Environmental interpretations of the Ajali Sandstone have suggested fluvial and flavio deltaic depositional model (Reyment, 1965; Murat, 1972; Hoque and Ezepue 1977; Banerjee, 1979), but a tidal depositional model was proposed by Ladipo (1986). The Nsukka Formation is a parallic sequence of coastal sandstone with beds of mudstone, shale, lenses of coal deposited in the lower paleocene.

Geo-electrical survey on the basal sandstone of the Nsukka Formation distinquished two and three layer earth (Mamah and Ekine, 1989). Mbuk et al, (1985) noted a decline in the number of specimens of dinoflagelletes across the Maastrichtian- Danian boundary of the Nsukka Formation while the permeability is between 2.0 - 20.7 x 10^{-10}cm/s (Mamah amd Ekine, 1989). Egboka (1983) suggest that the hydraulic conductivity of the Ajali sandstone is in the order of 1×10^{-12} cm/s.

CHAPTER TWO

GENERAL GEOLOGY

2.1 REGIONAL TECTONIC EVOLUTION AND SEDIMENTOLOGY

The study area is part of the Anambra Basin which is filled with the cretaceous sediments (see table 1). The Basin is one of the tectonic consequence from a formally lower Benue Trough (Nwachukwu, 1972; Murrat, 1972).

The Benue Trough, located at a major re-entrant in the West African continental margin, is a unique rift feature of the African continent in that it occupies an intra continental position and has a thick compressionally folded cretaceous supracrustal fill (Cratchley and Jones, 1965; Grant, 1971; Burke et al, 1971; Burke and Whiteman, 1973; Nwachukwu, 1972; Olade, 1975; Petters 1978). For this reason, its origin has been widely debated especially in relation to plate tectonics. The recent comparism of the Benue Trough with an allacogen by (Hoffman et al, 1974; Hoque and Nwajide, TABLE: 1

STRATIGRAPHIC RELATIONSHIP AND PETROLOGY OF SANDSTONES OF THE SOUTHERN NIGERIA SEDIMENTARY BASIN

(MODIFIED FROM HOQUE, 1976)

AGE	LITHOSTRATIGRAPHIC SEQUENCE	PETROLOGY OF SANDSTONE
EOCENE	Ameki Formation	
PALEOCENE	Imo Shale	
[illegible]	Nsukka Formation	[illegible]
	Ajali Sandstone	
	Mamu Formation	
Campanian	Nkporo/Enugu Shale	
Coniacian - Santonian	Awgu Shale	
Turonian Cenomanian	Eze-Aku Shale Odukpani Formation	[illegible]
Albian	Asu River Group	

1985) has furnished the most appropriate model so far to explain its origin and tectonic evolution. They expanded an earlier hypothesis by Burke et al, 1971; Olade, 1975 that the Benue Trough is a failed arm of three arm radial rift system. using the Athapuscow aulacogen of the Canadian shield as an example, the aulacogen model explains some of the salient structural features of the Benue Trough such as the broad down warping involving the basement and overlying sediments, and the general absence of clearly defined marginal faults where basement contacts have been mapped so far (Cratchley and Jones, 1965). The model also justifies consideration of the Anambra basin (see fig. 3) as part of the Benue Trough, being a related structure that developed after the compressional stage. Further, it offers a tectonic framework upon which to interprete the sedimentary history of the Benue Trough in order to arrive at some stratigraphic and paleogeographic synthesis (Petters, 1978).

Sedimentation in the Benue Trough which started during the early cretaceous was controlled by two dominant factors. One was the progressive eustatic rise in sea level from the Albian, leading to the wide spread drowing of continental

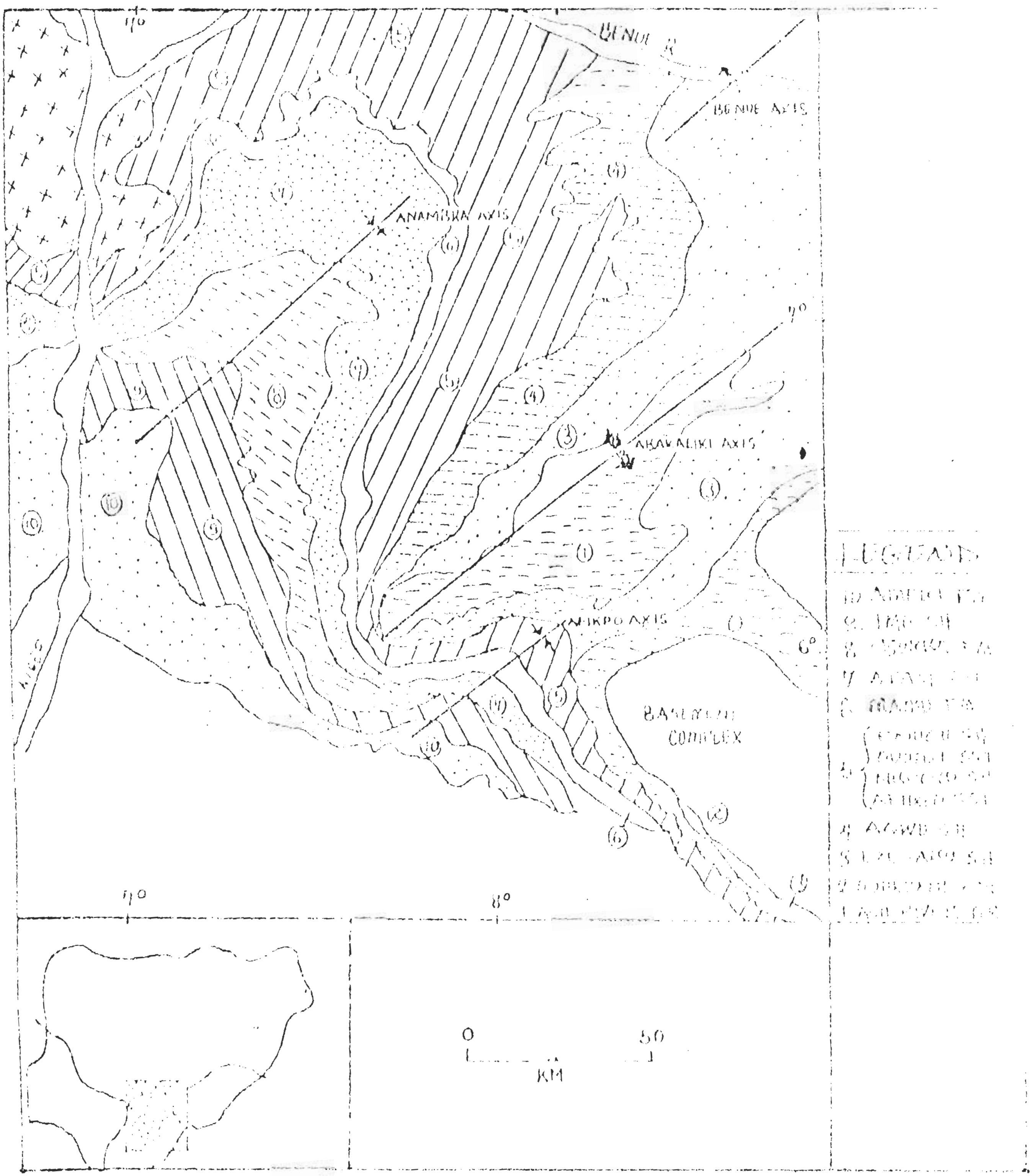

FIG. 3: GEOLOGIC MAP OF SOUTHEASTERN NIGERIA (AFTER HOQUE AND EZEPUE, 1977)

margins and the creation of vast interior sea ways during the Cenomanian and Turonian (Hoque, 1977; Hoque and Nwajide, 1985). The other is a local diastrophism. Both processes resulted in the trangressive-regressive cycles that characterized the depositional pattern in the Basin.

Three major unconformity-bounded depositional sequences can be recognized in the Benue trough. The oldest sequence represents the initial Albian-cenomanian transgressive pulse, followed by a Turonian-coniacian sequence, which represents the phase of maximum transgression. Then the campanian-maastrichtian post compressional sequence. Within these major stratigraphic units, there are deposits which reflect minor advances and retreats of the shoreline caused by either local tectonic movements or changes in the rate of sediment influx (Murat, 1972; Mode, 1991).

The oldest rock in the Southern Benue trough (refer to fig. 3) is the Abakaliki pyroclastics which were extruded during the graben phase (Hoque and Nwajide, 1985). This was followed by the Albian marine sediments of the Asu river group. Sedimentation continued under this initial cycle with the deposition of Ezeaku Formation until lower Santonian when the compressional stage was initiated. This led to the Formation of the Abakaliki anticlinorium at the Southern part of the trough and synclinorium by its flanks. The synclinorium formed the Anambra basin to the west and the Afikpo syncline to the eastern flank.

Sedimentation started in the Anambra basin after the tectonism with the campano-maastrichtian sediments of the Enugu Formation. This was followed successively by the maastrichtian sediments of the Mamu Formation, the Ajali sandstone and the Nsukka Formation.

The first depositional cycle (Albian to santonian) is characterized by lithic fills of feldspathic sandstones, while the second cycle which forms campanian to early Eocene is characterized by quartz arenites (Hoque, 1971).

2.2 REGIONAL LITHO STRATIGRAPHY UNITS

The project area is situated within the Anambra Basin and is underlain by rock Formations ranging in age from conician to Paleocene. The rocks include Mamu formation, Ajali Sandstone and Nsukka formation (maastrichtian in age). Nwajide, (1976).

The dominant lithologies in the area are sandstone, and shale. The sedimentary or stratigraphic subdivisions are based on variations in vertical associations of lithofacies.

2.2.1 Mamu Formation

Lithologically, the Mamu Formation consists of distinctive assemblage of sandstone shale, mudstone and sandy shale with coal seams at several horizons (Agagu et al 1985; Reyment 1965; Simpson 1954). The shales and mudstones are dark blue or grey and grade into the sandstones. Grey mudstones with scattered plant impressions grades into high carbonaceous shales. Carbonaceous materials is present in varying amounts and occurs as streaks on the bedding of the sandstones or as irregular ramifications (Reyment 1965). Dip values vary from $4^0 - 6^0$. The Formation is a parallic sequence deposited in a marginal environment probably in those of beaches, lagoons and swamps (Reyment, 1965; Reyment and Tait, 1983).

2.2.2 Ajali Sandstone

This overlies the Mamu Formation conformably and consists of thick friable, poorly consolidated sandstones, typically white in colour, but sometimes pinkish due to post depositional iron staining, with mudstones and shales as intercalations (Reyment 1965; Simpson 1954).

One of the most conspicuous feature of the Ajali sandstone is cross-stratification. These includes large scale herringbone, planer and trough crossbeddings. Ripple, cross lamination is common. Horizontal lamination is also preserved lenticular and flaser stratification is present. Leaf impressions are preserved in mudstone interbeds. The sandstone members are often overlain by a considerable thickness of red earth, or insitu laterite in places where Nsukka Formatoin has been eroded away (Hoque and Ezepue, 1977). The mean angle of the forest laminae with the underlying major bedding planes range from 18^0 to 20^0 in a west-south-west direction (Barnerjee 1979). Vertical burrow of organisms likely to be ichonofossils ophiormorpha or skolithos also occur in few places.

Environmental interpretation of the Ajali sandstone have suggested fluvial and fluvio-deltaic depositional model (Reyment 1965; Murat 1972; Ezepue and Hoque, 1977). However, a more recent work by Ladipo (1986) based on process interpretation of sedimentary structures and paleocurrent analysis have suggested a tidal shelf model for the southern region of the Formation.

2.2.3 Nsukka Formation

This overlies the Ajali sandstone conformably and occurs as residual hills on the underlying Ajali sandstone.

Lithologically, it consists of alternating succession of sandstone, dark shales and sandy shales with thin coal seams at various horizons. Thus it is similar to the Mamu Formation. The basal sandstone of the Nsukka Formation has a thickness of about 15m and it is present throughout Nsukka and most of Udi division (Reyment, 1965). It is succeeded by well-bedded blue clays. Fragmentary plant remains are abundant in the Formation and where the carbonaceous shales have been ferruginized in the zone of laterization, leaf impressions are preserved. The dip amount of the units vary between 3^0 and 4^0 (Simpson, 1954; Reyment 1965). The environment of deposition is similar to that of Mamu formation.

2.3 SUBSURFACE GEOLOGY OF NSUKKA AREA

Subsurface geological data from borehole lithologic log of U.N.N reveal that the project area stands on sandstone undergoing laterization (fig. 4). This is the basal unit of the Nsukka Formation (Reyment, 1965; Mamah and Ekine 1989). The unit can be regarded as impervious due to the effects of weathering where iron oxide forms the matrix. It is mineralogically mature with abundant quartz (75 – 95%)

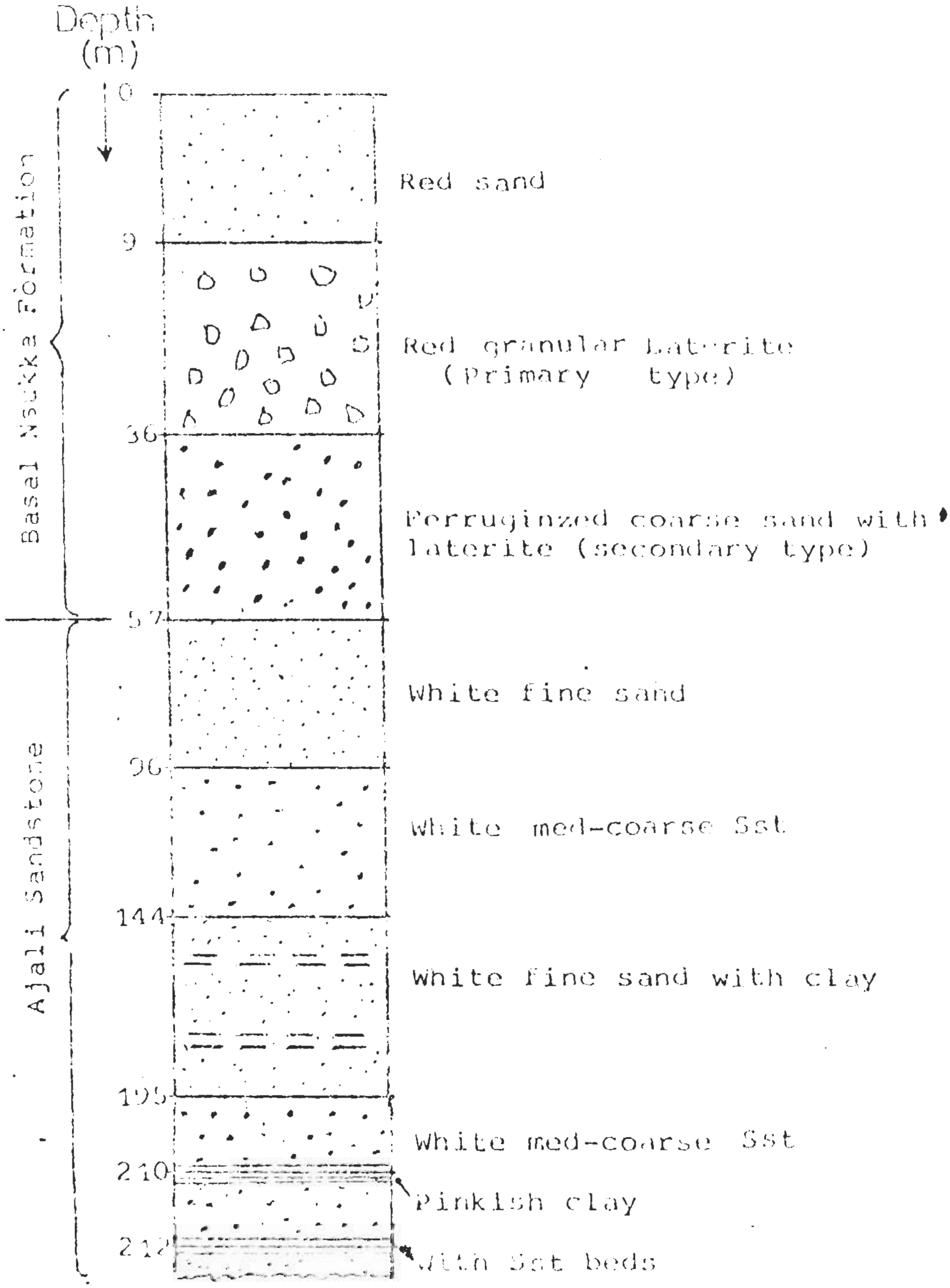

Fig: 4 (Lithologic log of U.N.N. New borehole)
(Courtesy of the Works Dept. U.N.N.)

An upwards fining sequence in the unit is indicative of transgressive period while the prominent quartz is indicative of tidal flat environment.

and 5 15% matrix (Mamah and Ekine 1989). Pullan (1967) in Mamah and Ekine (1989) classified Nigerian laterites into two broad genetic groups, vix primary and secondary. The primary type (vesicular, vermicular and cellular) predominate in the basal sandstone. The secondary laterite which is mostly recemented fine detrital materials form as a result of enrichment by vertical solution transport and or lateral solution transport. This forms the transition zone between the basal Nsukka Formation and the underlying Ajali sandstone.

Chemical analysis shows that the laterites are low in Na_2Co_3, K_2O, CaO and P_2O_5 but high in Fe_2O_3, Al_2O_3 (Petel et al 1976). The iron oxide content tend to decrease with depth. This trend is reflected by the decrease of Schellman's (1983) weathering ratio (RW) with depth. The range of RW (.26 1.59) show that lateritization is moderate (Mamah and Ekine, 1989).

CHAPTER THREE

INTRODUCTION TO RESISTIVITY METHOD

3.1 PREAMBLE

Electrical resistivity method studies horizontal and vertical variations in electrical conductivity of the earth. Electrical potential is generated by introducing direct or low frequency alternating current into the earth through point electrode placed on the surface. The voltage signature of the ground is obtained through another point electrodes placed in the vicinity of the current electrode.

3.2 EQUIPMENT FOR ELECTRICAL RESISTIVITY WORK

The basic equipment for carrying resistivity measurements includes; a power source (either direct current of low frequency alternating current), meteres for measuring current and voltages,electrodes,cables and rods. A low frequency sine wave transistor osillator with transformer output of a few watts makes a convenient portable sources. (Telford et al, 1978)

The equipment is set up as shown in (fig 5) direction of current flow and equipotential lines everywhere on the subsurface is a function of resistivity of the subsurface. They are always at any time and position re-orient themselves so as to maintain a right angle with current lines. Depth of penetration of current depends on factors such as; subsurface geology and electrode spacing. The Larger the spacing the deeper the current penetration.

3.3 THEORITICAL BASIS

From ohms law, the resistivity of any material can be defined as the resistance in ohms between the opposite faces of a unit cube of the material. For a uniform and conducting cylinder

$$\varrho = \frac{\partial R \partial A}{\partial L} \quad \text{-------------- Equation 3.1}$$

Where ϱ = resistivity

∂R = the resistance of the cylinder

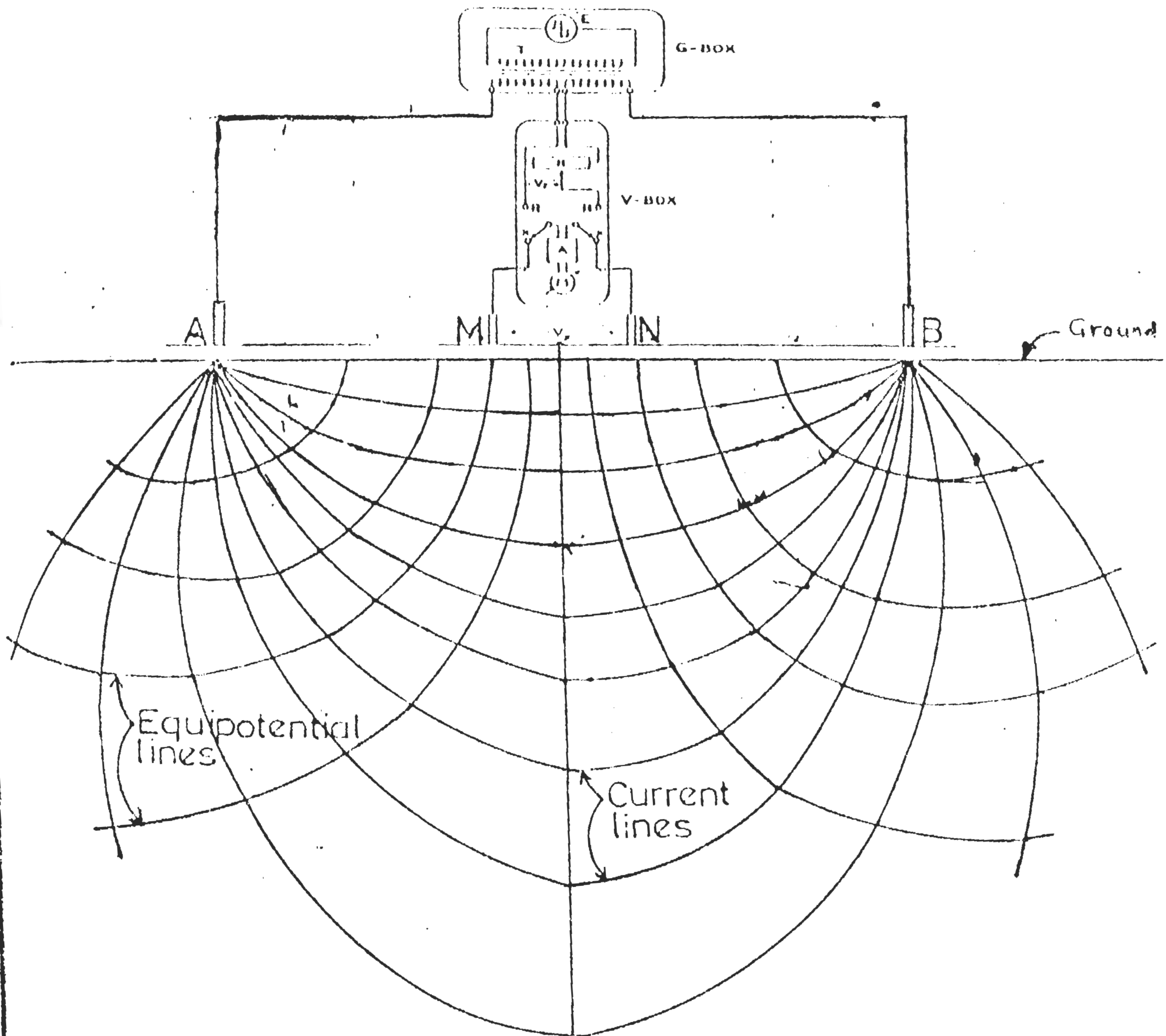

Fig. 5 The arrangement of resistivity measuring instrument showing potential-lines and current lines. A and B illustrate current-electrodes while M and N are potential-electrodes. (Modified from Telford et. al., 1978; Parasnis 1962)

∂L = Length

∂A = cross sectional area.

It has been proven by many workers that the current density in any direction within a material is given by the negative partial derivative of the potential gradient in that direction divided by the resistivity

$$\varrho_i = \frac{-\partial v}{\partial L} \text{ .... Equation 3.2}$$

Where ϱ = resistivity of the material.

i= current density

$\frac{\partial v}{\partial L}$ = potential gradient

For a single current electrode on the surface of a homogenous material of resistivity, the current is completed by a current sink at a large distance from the electrode, so the current distribution is uniform over hemispherical shells centered on surface at a distance 'r' from the electrode (see fig 6). The shell has a surface area of $2\pi r^2 m^2$, therefore the current density will be given as

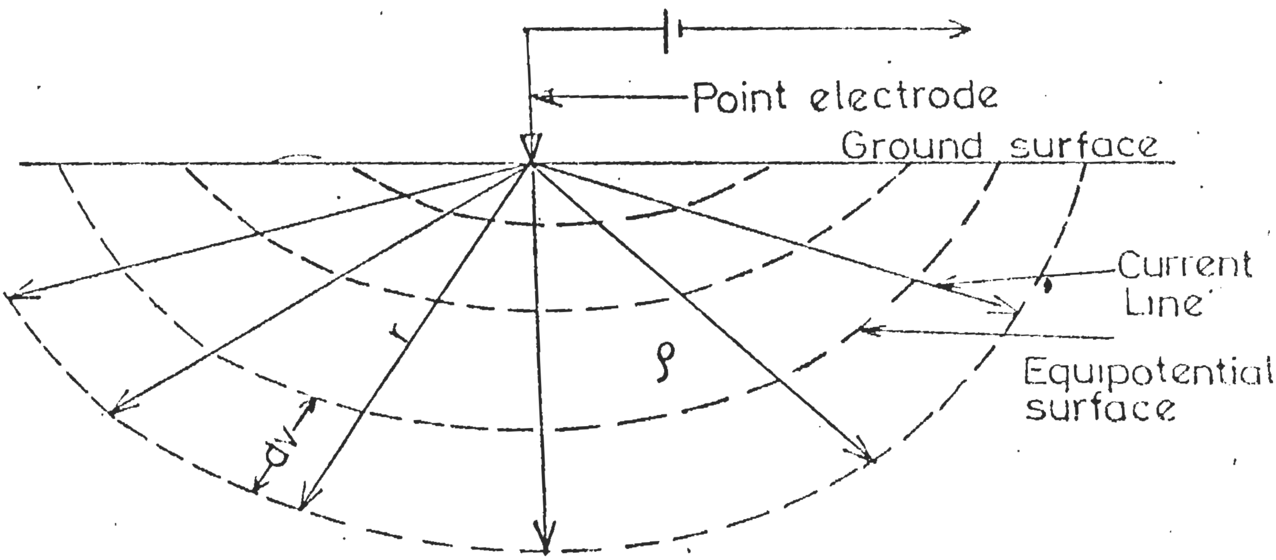

Fig: 6 (A single current electrode on the surface of a homogeneous material of resistivity ρ)
After Keary and Brooks 1984

$j = \frac{1}{2}\pi r^2$ ....equation 3.3

then the potential gradient associated with this current density is

$$\frac{dv}{dr} = -\varrho j = \frac{-\varrho i}{2\pi r^2}$$ ....equation 3.4

the potential 'Vr' at distance 'V' is then obtained by integration

$$vr = \int dv = -\int \frac{\varrho I dr}{2\pi r^2} = \frac{\varrho I}{2\pi r}$$ .... equation 3.5

If we apply this to a two point electrode (as shown bellow fig 7). The potential at the electrode ' M' will be

$$Vrm = \frac{\varrho_1}{2\pi r} - \frac{\varrho I}{2\pi r_2} = \frac{\varrho I}{2\pi r}\left(\frac{1}{r_1} - \frac{1}{r_1}\right)$$ .... equation 3.6

The potential at the electrode 'N' will be

$$VrN \quad \frac{\varrho I}{2\pi}\left(\frac{1}{r_3} - \frac{1}{r_4}\right)$$ .... equation 3.7

So that the potential difference measured will be

$$\Delta V = Vrm - VrN = \frac{\varrho_1}{2\pi}\left\{\left(\frac{1}{r_1} - \frac{1}{r_2}\right) - \left(\frac{1}{r_3} - \frac{1}{r_4}\right)\right\}$$ ... Equation 3.8

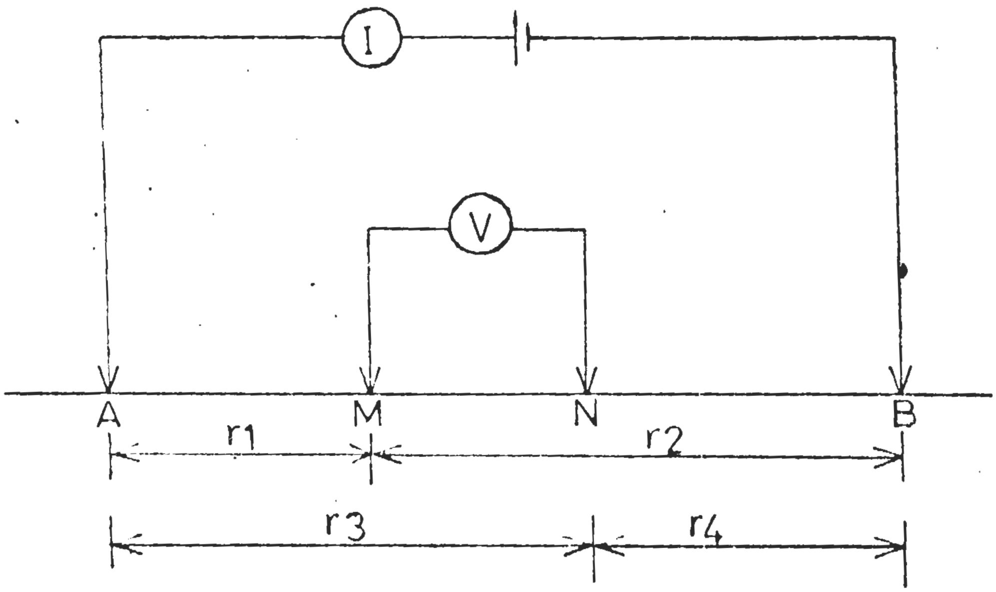

Fig:7 (Theoretical electrode arrangement showing the dimensions of electrode spacings for a given CONFIGURATION)
After Dobrin and Savit 1988.

The resistivity of the medium will be given as

$$\varrho = \frac{2\pi \Delta v}{I} \left\{ \frac{1}{\left(\frac{1}{r_1} - \frac{1}{r_2}\right) - \left(\frac{1}{r_3} - \frac{1}{r_4}\right)} \right\} \qquad \text{..................} \; 3.9$$

$$P = 2\pi \frac{\Delta V}{I} G \qquad \text{..................} \; 3.10$$

$$\text{Where } G = \left\{ \frac{1}{\left(\frac{1}{r_1} - \frac{1}{r_2}\right) - \left(\frac{1}{r_3} - \frac{1}{r_4}\right)} \right\} \qquad \text{..............} \; 3.11$$

This is known as geometrical factor and it is a function of electrode configuration. Because the earth is never homogeneous, resistivity is usually defined as apparent resis tivity ϱa.

3.4 ELECTRODE CONFIGURATION

The are many forms of electrode arrangements in resistivity field work, each having a peculiar field procedure and method of data interpretation. Two arrangements are very popular namely; wenner and schlumberger electrode arrangements.

3.4.1 Wenner Configuration

In Wenner arrangement, equal spacing are maintained between the four electrodes in a line.(see fig 8). This will imply that the potential electrode spacing MN is always a one-third of the current electrode spacing AB.

Using equation 3.11 we can express the apparent resistivity of this configuration as:

$$\rho a = 2\pi a \frac{\Delta V}{I} \quad \ldots\ldots\ldots 3.12$$

3.4.2 Schlumberger Configuration

The current electrodes spacing are further apart than the potential electrode-spacing, we can have symmetrical or asymmetrical arrangement. For

Wenner Configuration

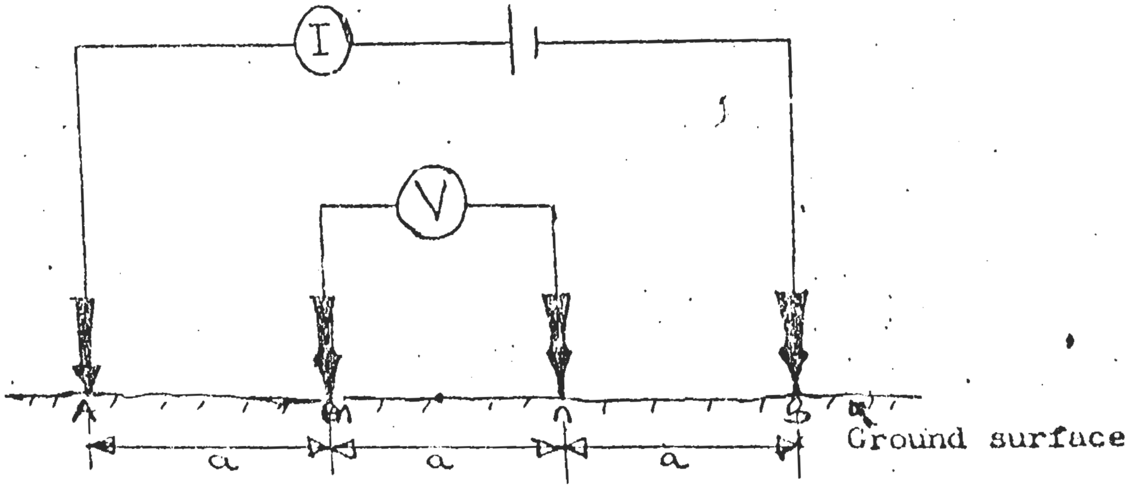

fig:8 (Theoretical field set up of Wenner electrode arrangement After Parasnis D.S. 1962).

symmetrical arrangement, the potential and current electrodes share common midpoint, while for asymmetrical arrangement, the two sets of electrodes do not share common midpoint. (see fig. 9).

3.5 **TECHNIQUES**

Two techniques for applying any configuration method can be distinguished, namely 'traversing' (Horizontal profiling) and 'probing' (vertical electrical sounding). In the former, electrode spacing 'A' is held constant and the system as a whole is moved over the surface of the earth. The movement is made either along the line of the electrodes (longitudinal traversing) or perpendicular to it (tranverse traversing). In the expanding electrode probe the line of the electrodes is fixed in direction and spacing 'A' varied, keeping the centre of the electrode line at the same point.

The method of traversing is used to determine the variations in the apparent resistivity in a horizontal direction within a pre-selected depth range. The method is particularly useful

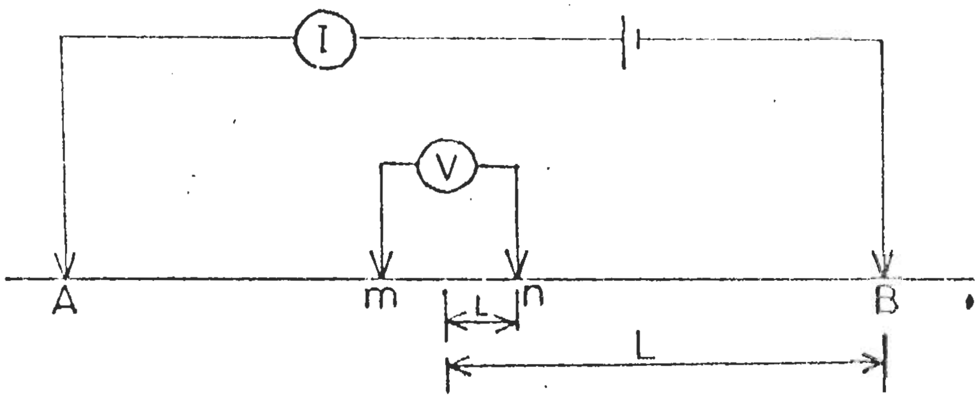

Fig: 9 (Symmetrical schlumberger electrode configuration)

$$l = \frac{mn}{2}$$

$$L = \frac{AB}{2}$$

for recognisance surveys in structural prospecting for contacts, dykes, faults and fissure zones. It may be applied to trace the boundary of intruding sea-water, in favourable conditions it can be used for delineation of gravel lenses embedded in clayey material and for the detection of depressions in the surface of dense bedrock.

The method of probing furnishes detailed information on the vertical succession of different conducting zones and their individual thickness and true resistivities. For this reason, the method is particularly valuable for investigations on horizontally or nearly horizontally stratified ground.

CHAPTER FOUR

INTRODUCTION TO MAGNETIC METHOD

4.1 PREAMBLE

Magnetic surveying is one of the most widely used geophysical methods in terms of line length survey. It is a rapid and cost effective technique for locating both hidden ores and structures associated with mineral deposits.

4.2 MAGNETIC EQUIPMENT

A flux-gate type magnetometer which measures the Z-component (vertical magnetic component of the magnetic field). Fig. 10 illustrates how the field is measured. Two parallel cores, each with a magnetization curve of the type shown at the upper left are alligned with their axis in the direction of the earth's field. Primary coils in the series magnatize the two cores with same flux density but in opposite directions since they are wound oppositely around the respective cores. The earth's field at any given instance reinforces the field set up

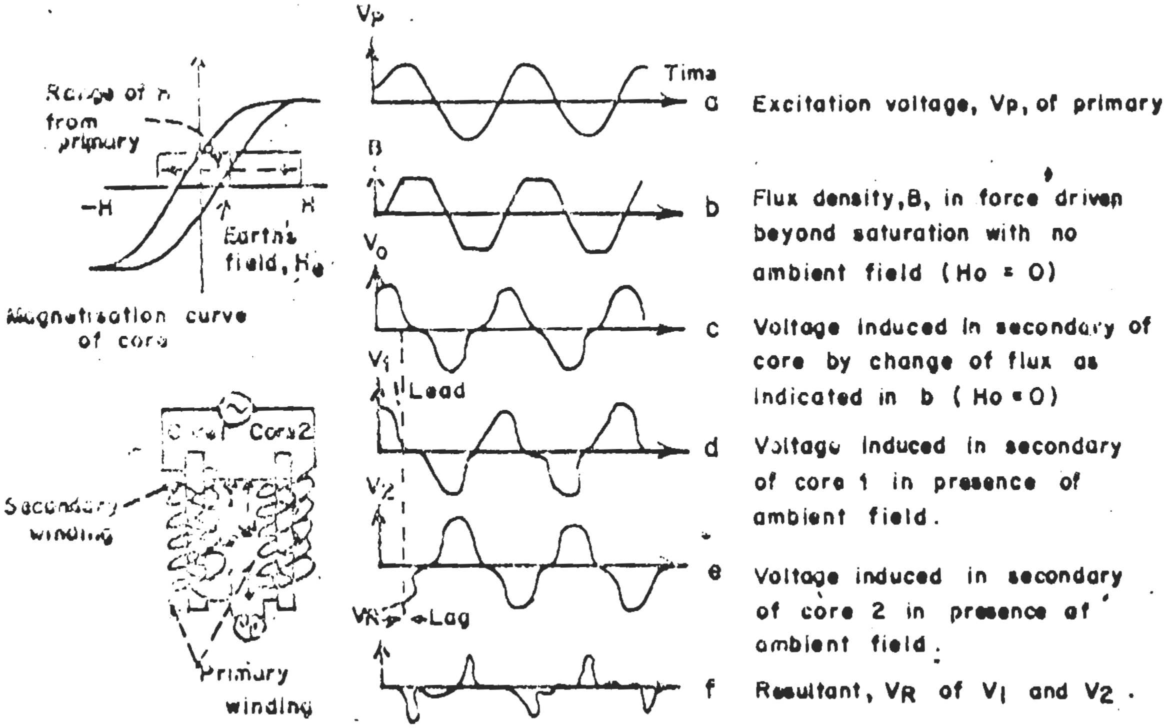

Fig: 10. Principle of the flux-gate magnetometer.
(AFTER DOBRIN, 1976)

by one of the coils and opposes the field of the other. Each coil has in addition a secondary winding, the two secondaries being connected to a voltameter that reads the difference of the two outputs (Dobrin, 1976).

Consider the magnetization of a single core in the absence of an amblient field (as when the core's axis is normal to the earths field). The sinusoidal exciting field H (see curve 'a' of fig. 10) drives the core past saturation at the top and bottom of each cycle (as shown by the truncated peaks in curve 'b'). The secondary voltage is proportional to the rate of change of magnetic flux and thus will dip towards zero during the portion of the cycle when the core is saturated (as in curve 'c').

If the ambient is introduced which aids the magnetization from the existing current, the saturation point, as indicated by the dip in the secondary voltage, is reached earlier in cycle than it would be in the presence of an ambient field opposing the exciting field (curves 'd' and 'e'). If the voltage outputs of both coils are connected in opposition, the resultant output (curve f) consists of pairs of pips as shown.

The height of the pips is within reasonable limits, proportional to the ambient magnetic field.

4.3 APPLICABILITY OF MAGNETIC SURVEYING

Sharma (1987) reported that roughly about 60% of magnetic surveys are carried out for regional geological mapping and mineral exploration purposes, the remainder being mainly for petroleum exploration. For mineral exploration, mineral deposits such as magnetite, illmenite, pyrrhotite and to a lesser extent, haematite can give rise to major magnetic anomalies. Manganese and chromium ores may also produce detectable anomalies. Other ore minerals, themselves non-magnetic may be associated with magnetic rocks for example, the occurrence of gold in intrusive igneous rocks or diamonds in kimberlite pipes. Domzalski (1958) pointed out that the aeromagnetic anomalies reflect the location of rocks with high concentrations of niobium minerals. On a smaller scale, ground magnetic surveying is often of use to the engineering geologist and hydrogeologist in locating buried features such as subsurface contacts in the basement, faults and dykes. It may also be applied to archeological and geotechnical investigation for the location of buried man-made ferrous objects.

Magnetic prospecting needs instruments with very high sensitivity, high speed, good spatial resolution and perfect reduction of external disturbances.

A major use of magnetic surveying is an aid to geological mapping over extensive regions with a thick sedimentary cover, structural features may be revealed if magnetic horizons such as ferruginous sandstone and shales, tuffs and lava flow are present within the sedimentary sequence. In the absence of magnetic sediments, magnetic survey data can provide information on the nature and form of the crystalline basement. In academic studies, the magnetic method can be used to provide information on geological structures at all scales.

CHAPTER FIVE

5.0 INSTRUMENTATION USED/PRECAUTIONS

5.1 INSTRUMENTATION USED FOR RESISTIVITY SURVEY

The method of resistivity work employed for this project was entirely traversing (horizontal profiling). The basic instrument is the Abem Terrameter which is made up of a V-box and a G-box. Others may include four stainless electrodes, four rolls of connecting cables, hammer and measuring tapes.

The instrument is suitable for use in structural investigations down to depths of 600 meters when the resistivity of the subsurface is not below 50 ohm-meters.

The equipment uses internally fitted standard batteries. The G-box uses twelve 1.5 volts (each) standard tourch batteries. The G-box contains the current supply circuit consisting of transistorized oscillator (AC – DC Converter) with batteries and operating controls. It is connected to the outer current electrodes and also takes current from the V-box. The V-box holds the circuit necessary to measure the resistivity of the ground. It is connected to the inner potential electrodes and it takes current from the G-box right inside the ground at position market 'X' of the 'X – R' switch on the box, at a position 'R' of the switch, current goes to the electrodes and the potentiometer.The resistivity value at the position of measurement is obtained from the formula for the wenner configuration.

$\kappa_a = 2\pi QR$

where

κ_a	=	Apparent resistivity (ohm-m)
Q	=	Centre-spread distance (m)
R	=	Resistance (ohms)
π	=	3.14 constant

Further, special characteristics of a terrameter may include the following:

a. It has a good sensitivity and high instrumental accuracy, +3% for readings as low as 0.003 ohm/m and +10% for readings of 0.01 ohm/m.

b. The use of a very low frequency square wave alternating current to create the potential difference avoids difficulties due to electrode polarization and reduces capacitive effects to a minimum.

c. The use of two separate units, one for current supply and the other for measurement eliminates the possibility of current leakage between the oscillator and voltmeter circuits.

5.2 THE INSTRUMENTATION USED, FOR MAGNETIC SURVEY

The magnetic instrument used in the flux gate-type magnetometer, which measures the Z-component (vertical magnetic component). Two parallel cores each with a magnetization curve are aligned with their axis in the direction of the earth's field. Primary coils in the series magnetise the two cores with the same flux density but in opposite directions, since they are wound appositely around the respective cores. The earth's field at any given instant reinforces the field set up by one of the coils and opposes the field of the other. Each coil has, in addition, a secondary winding, the two secondaries being connected to a voltmeter that reads the difference of the two outputs (Dobrin, 1976).

5.3 PRECAUTIONS

The precautions taken for both the resistivity and magnetic measurement includes: For the resistivity measurement:

i. Saline water was poured on the position of the electrodes, especially the current electrodes in order to reduce the contact resistance between the electrodes and the ground.
ii. The current electrodes are hammered deep down into the ground (about 15 cm deep) for good electrical contact with the ground.
iii. The V-box and G-box were kept at a maximum separation of 50cm with their short sides facing each other.
iv. The cables were not allowed to touch or run parallel for a long distance.

v. The reels of the potential cables were oriented in such a way that they were made perpendicular to the current cables.

Note the precautions (iii), (iv) and (v) were done to avoid induction effects.

vi. The electrodes are made of stainless steel and about 30cm long. The platinum electrodes make it possible to avoid electrochemical forces produced between the metal electrodes and the ground and also avoid corrosion.

vii. Current oscillator was switched off after each measurement and the connecting cables disconnected from the reels of wires before any change of position was made; to avoid accidents due to high voltage; to save batteries and to avoid damage to cables when positions were changed.

viii. The traverses were run along suitably selected straight profiles.

For the magnetic measurements, the precautions taken were:

i. We made sure that the 'bulls-eye' bubble was centered.

ii. After every reading, current was switched off to avoid running down of the batteries.

iii. Metallic objects that could influence the magnetic readings were not allowed in the vicinity of measurement.

iv. Two sets of readings for each station were done and the average taken. This was done by taking readings both in the east and west directions.

CHAPTER SIX

DATA ACQUISITION/ANALYSIS

The field work was carried out intermittently between the months of June to November 2000, during this period both the electrical resistivity and magnetic methods were employed.

6.1 RESISTIVITY AND MAGNETIC SURVEY

6.1.1 Electrical Resistivity Survey

Seven resistivity profiles (NSK/RS 1 – 7) as shown in Figures (11 – 17) were obtained. The profile length are between 900m and 1000m (1km) each. Essentially the profile lengths were run along the grid line as shown on the base map with the exception of NSK/RS3 profile line running perpendicular (refer to Figs. 1a and 1b in the pocket at the last page).

Robert (1973) noted that since any subsurface discontinuity within the range of resistivity equipment may cause variation in the resistivity, it is important to consider the variations that are likely to be caused by faults in the earth's crust. He further stated that in steeply dipping faults, the resistivity properties may be divided into three distinct parts; viz, the resistivity of the blocks on each side of the fault and the resistivity of the fault zone itself. Various combinations are possible for example:

1. The resistivity of the two blocks and the fault zone may be unequal.
2. The two blocks may be of equal resistivity while the fault zone between them is either more resistive or more conductive than are the blocks. However, it is known in nature that a fault zone rarely consists of a simple homogeneous material whose resistivity is uniform but more commonly consisting of materials that differ greatly in resistivity.

From the resistivity profiles, it can be observed that both Resistivity highs and lows exist; the former is indicative of low conductive materials, e.g. laterite, dry sand etc while the latter is indicative of high conductive materials e.g. shales, clay, etc.

A depth penetration of 5(m) was inferred for the horizontal profiling, which implied that only the resistivity contrast within that depth "window" can be detected by the equipment. Using the Wenner configuration, the electrode separation was selected as 5m's apart. Note that this is also applicable to profiles NSK/RS2, NSK/RS3 and NSK/RS4 respectively (refer to Figs 1a and 1b in the pocket at the last page).

Further, it is assumed from the principles of resistivity profiling that an anomaly that indicates a fault or fracture is manifested by an abrupt contrast in resistivity values along the traverse lines.

6.1.1 (a) Profile NSK/RS1

The apparent resistivity readings from the field for NSK/RS1 were plotted against the center spread in meters as shown in (fig. 11 and table 2). The profile is along Ibeagwa Road on a bearing of 334^0.

Table 2 **Resistivity Survey**

Traverse: NSK/RS1

Location: Ibeagwa Road

Bearing: 334^0

S/No.	Distance (M)	ϱ_a (Ohm – Meters)
1	15	18.86
2	30	32.62
3	45	70.72
4	60	66.00
5	75	121.16
6	90	145.39
7	105	170.95
8	120	199.89
9	135	225.73
10	150	350.76
11	165	385.83
12	180	422.04
13	195	457.21
14	210	504.26
15	225	113.14
16	240	120.69
17	255	238.84
18	270	480.31
19	285	318.89
20	300	335.67
21	315	221.77
22	330	232.33
23	345	394.69
24	360	341.71

Table 2 Cont.

25	375	379.52
26	390	433.92
27	405	450.61
28	420	322.09
29	435	456.65
30	450	446.93
31	465	385.83
32	480	362.07
33	495	392.05
34	510	650.79
35	525	491.72
36	540	458.25
37	555	732.63
38	570	827.68
39	585	849.46
40	600	878.78
41	615	947.14
42	630	1294.98
43	645	1285.27
44	660	1783.97
45	675	1642.06
46	690	1977.82
47	705	1506.75
48	720	1846.58
49	735	600.63
50	750	990.05
51	765	1009.85
52	780	2294.64
53	795	2558.65
54	810	2606.93
55	825	2748.55

Table 2 Cont.

56	840	1742.47
57	855	2069.19
58	870	2280.49
59	885	2670.29
60	900	1357.77
61	915	1437.92
62	930	2104.55
63	945	2138.49
64	960	2172.44
65	975	2886.69
66	990	3435.17
67	1005	3487.22
68	1020	2532.63
69	1035	3187.94
70	1050	2772.13

FIG. II. RESISTIVITY SURVEY
TRAVERSE : NSK/RS1
LOCATION. IBEAGWA ROAD

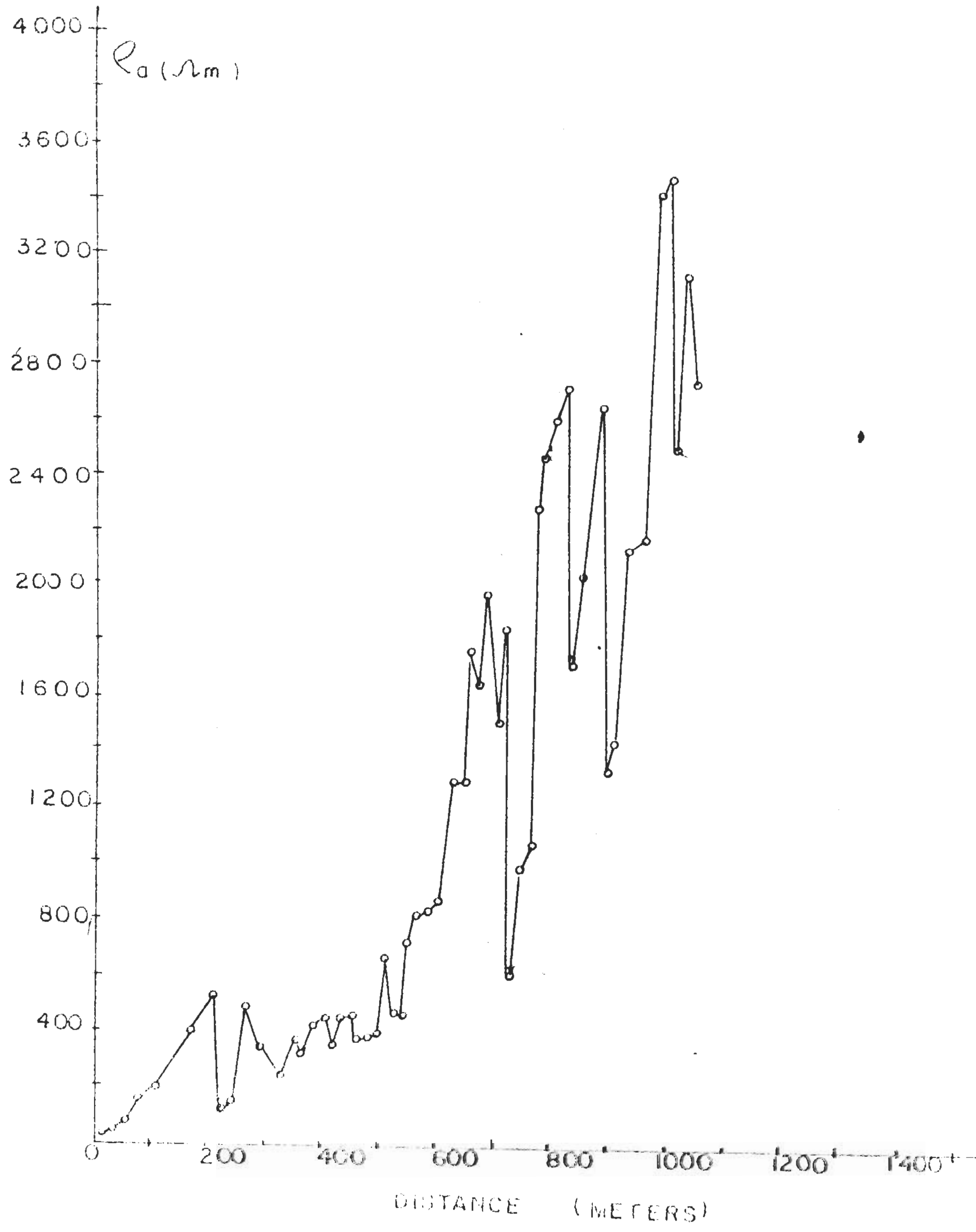

The profile length is 1050m's (1.050km) refer to Figs 1a and 1b in the pocket at the last page. There is resistivity high between 615m and 720m, 750m and 1050m, resistivity values show a form of ascending sequence, while distortions and low resistivity values exist between 15m and 600m respectively. The high resistivity values within the area may be indicative of low porosity area, low conductive materials, consolidated materials and no fracturing or faulting. While the low resistivity values is indicative of high porosity with loose materials and high conductive materials as well as the presence of structures probably a fault, fracture or joint sets.

6.1.1(b) Profile NSK/RS2

The survey was carried out opposite NSK/RS1 (refer to fig. 1) on a bearing of 124^0. A total of 255m distance was covered. The apparent resistivity readings got were plotted against distance (see fig. 12 and table 3).

From the profile high resistivity values were observed between 150m and 240m with a sharp drop at 255m

Table 3 Resistivity Survey

Traverse: NSK/RS2

Location: Opposite NSK/RS1

Bearing: 124^0

S/No.	Distance (M)	ϱ_a (Ohm – Meters)
1	15	10.84
2	30	18.86
3	45	50.35
4	60	77.32
5	75	88.63
6	90	82.03
7	105	151.81
8	120	107.11
9	135	118.81
10	150	311.16
11	165	252.04
12	180	272.69
13	195	297.86
14	210	319.45
15	225	342.27
16	240	366.59
17	255	227.62

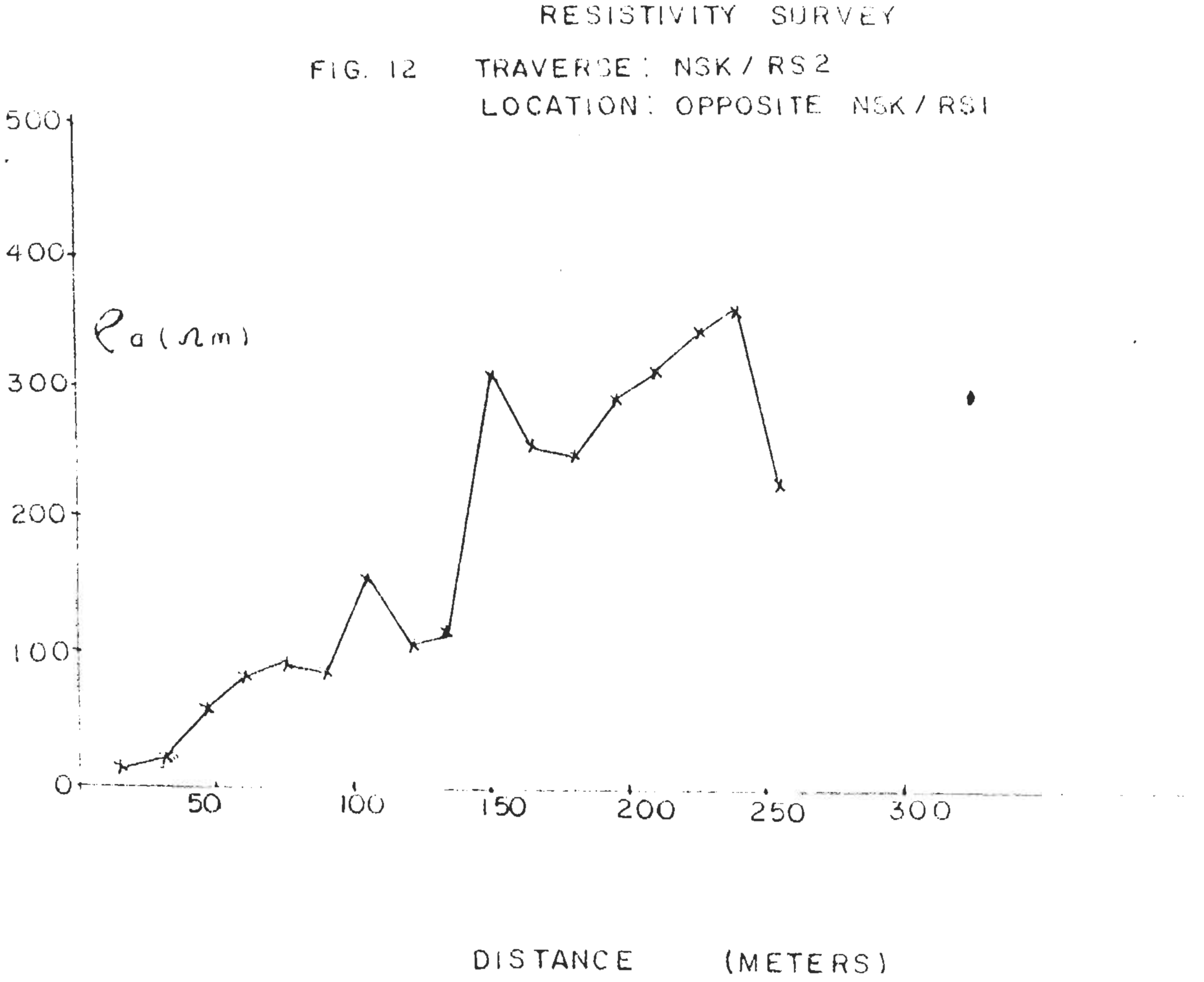
RESISTIVITY SURVEY
FIG. 12 TRAVERSE: NSK / RS2
LOCATION: OPPOSITE NSK / RS1
ρa (Ωm)
500
400
300
200
100
0
50
100
150
200
250
300
DISTANCE (METERS)

distance. This high values indicate that the area or region have low conductive materials, while low resistivity values were observed between a distance of 15m and 135m indicative of high conductivity region. Further slight distortions exist between 15m and 135m distance probably indicating a kind of joint set. It can be observed from the profile that the apparent resistivity values tend to increase in an ascending but gradual form.

6.1.1(c) Profile NSK/RS3

The survey was carried out on a perpendicular direction to NSK/RS2, on a bearing of 55^0. A total distance of 225m was covered. The apparent resistivity values was plotted against distance (see fig. 13 and table 4), and from the graph apparent resistivity values tend to increase in an ascending pattern with low resistivity value ranging between 15m and 90m and high values continuing from 105m to 225m. Essentially, the interpretation given for high and low resistivity values in previous interpretations is applicable to this profile.

Table 4 **Resistivity Survey**

Traverse: NSK/RS3

Location: Perpendicular to NSK/RS2

Bearing: 55^0

S/No.	Distance (M)	ϱ_a (Ohm – Meters)
1	15	28.76
2	30	81.84
3	45	111.73
4	60	192.35
5	75	206.49
6	90	249.09
7	105	351.79
8	120	401.29
9	135	369.99
10	150	502.56
11	165	550.71
12	180	494.46
13	195	533.21
14	210	574.23
15	225	753.85

RESISTIVITY SURVEY

FIG. 13: TRAVERSE: NSK/RS3

LOCATION: PERPENDICULAR TO NSK/RS2

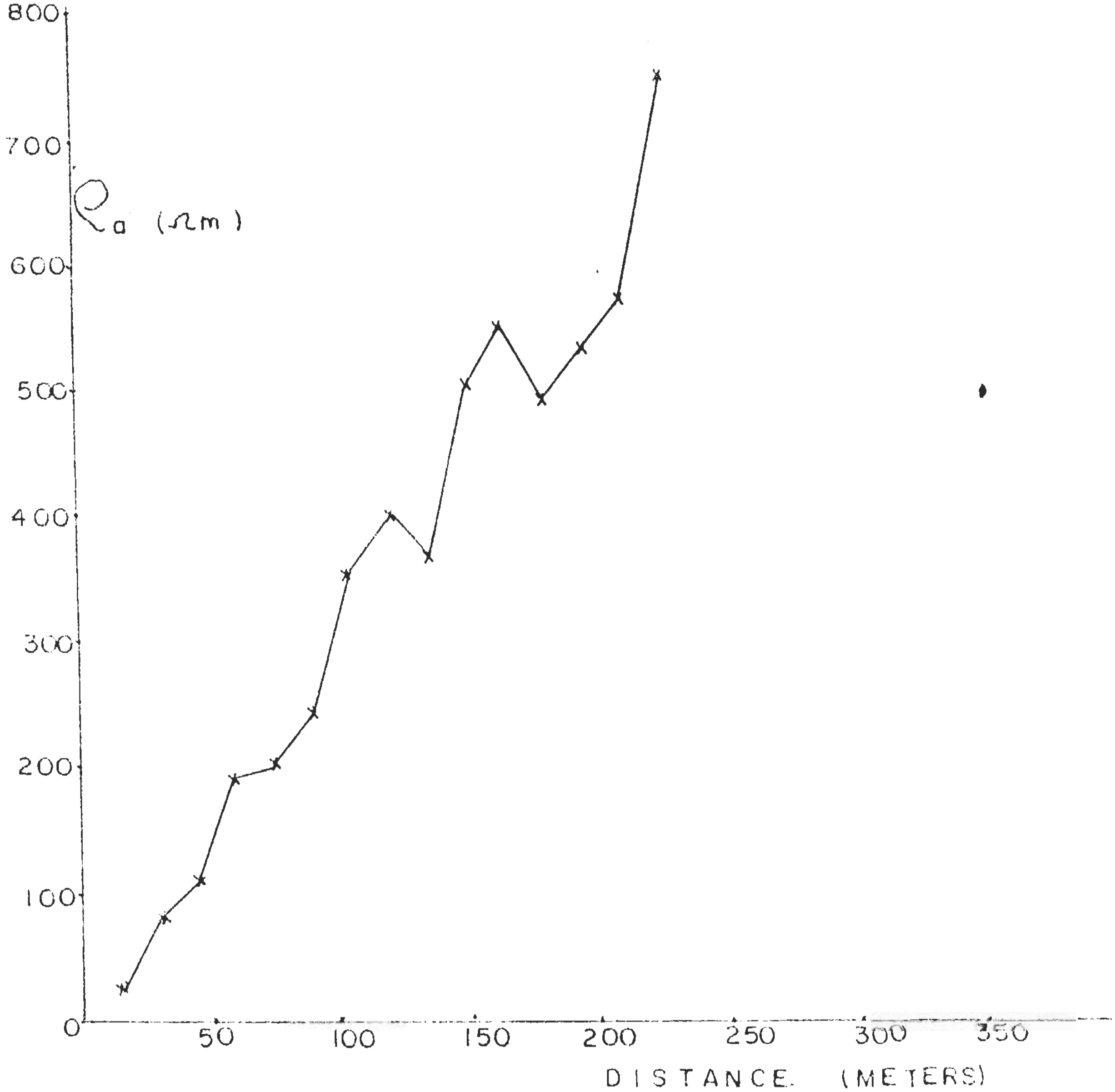

6.1.1(d) Profile NSK/RS4

The profile was carried out at a distance of 105m from profile NSK/RS2 on a bearing of 110^0 and a distance of 375m was covered (refer to fig. 1). A depth control of 5m was chosen and the apparent resistivity values got were plotted against distance. (Fig. 14 and table 5) from the profile the resistivity values trend in an ascending form with low and high values of resistivity present. The low values are within the range of 15m to 120m while the high values ascend from 135m to 375m, between 210m and 345m there is a linear projection of resistivity values and then a sharp increase at 360m. The interpretation for the high and low values in this profile are similar to previous interpretations.

6.1.1(e) Profile NSK/RS5

This profile was carried out at the University poultry road (U.N.N) on a bearing of 139^0 Azimuth, a total distance of 930m's was covered. The apparent resistivity readings were plotted against center spread in meters as shown in (Fig. 15 and Table 6).

Table 5 **Resistivity Survey**

Traverse: NSK/RS4

Location: 105m from NSK/RS2

Bearing: 110^0

S/No.	Distance (M)	ρ_a (Ohm – Meters)
1	15	62.04
2	30	152.18
3	45	151.34
4	60	199.89
5	75	249.87
6	90	268.73
7	105	211.21
8	120	241.38
9	135	396.30
10	150	440.33
11	165	486.44
12	180	599.68
13	195	759.98
14	210	1023.05
15	225	1097.54
16	240	1169.19
17	255	993.82
18	270	1053.95
19	285	1112.53
20	300	999.47
21	315	1049.45
22	330	972.88
23	345	1017.12
24	360	1403.04
25	375	1826.87

RESISTIVITY SURVEY

FIG 14: TRAVERSE: NSK/RS4

LOCATION: 105 METERS FROM NSK/RS2

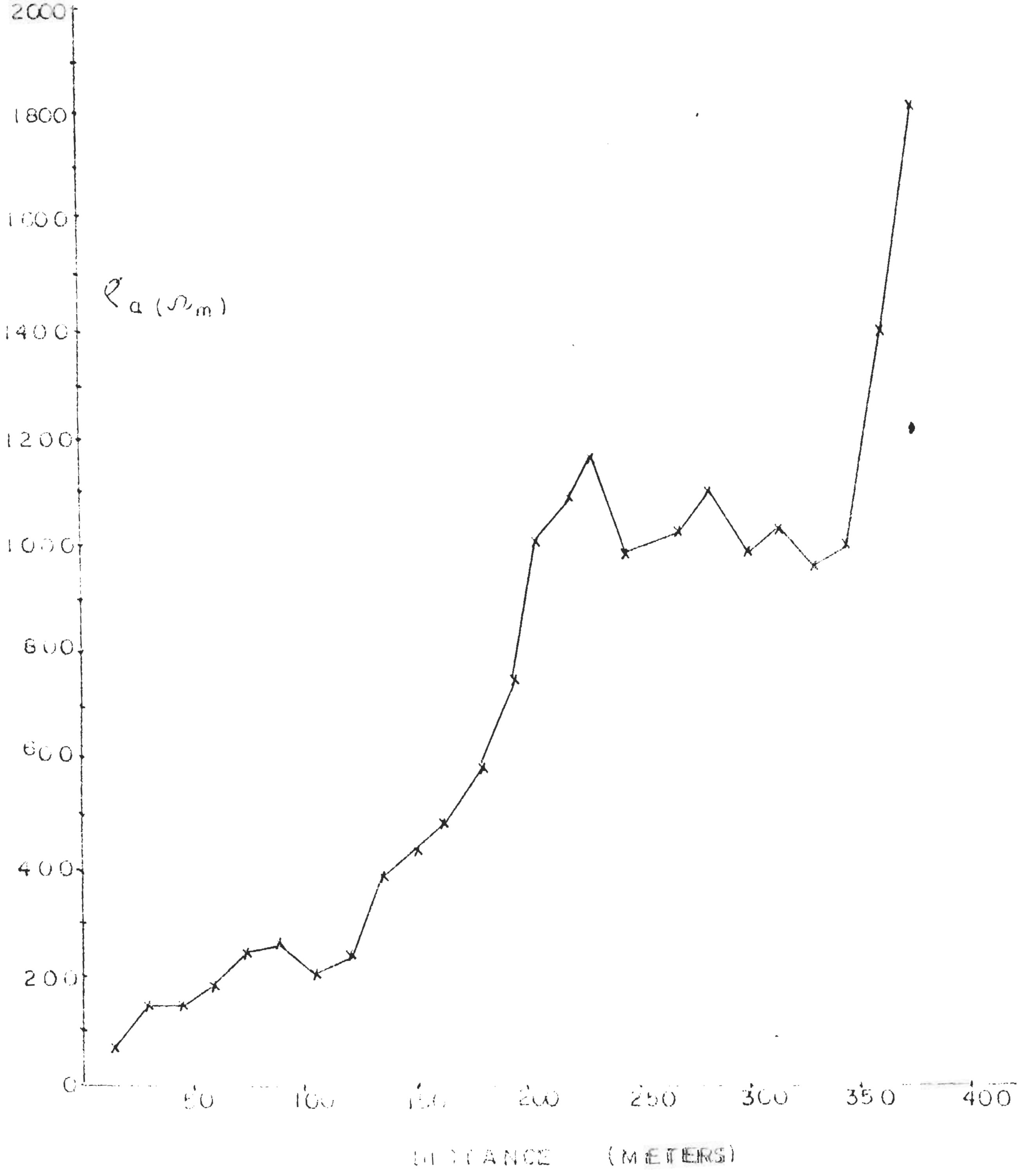

Table 6 Resistivity Survey

Traverse: NSK/RS5

Location: University Poultry Road

Bearing: 139^0

S/No.	Distance (M)	ϱ_a (Ohm – Meters)
1	30	34.32
2	60	125.97
3	90	264.77
4	120	440.52
5	150	504.45
6	180	554.43
7	210	571.59
8	240	653.24
9	270	999.66
10	300	839.18
11	330	472.96
12	360	529.53
13	390	375.09
14	420	609.87
15	450	806.18

Table 6 Cont.

16	480	1798.29
17	510	1929.93
18	540	2206.39
19	570	1415.29
20	600	1719.85
21	630	879.16
22	660	360.94
23	690	967.23
24	720	2688.39
25	750	1291.77
26	780	1181.64
27	810	626.27
28	840	248.17
29	870	448.44
30	900	311.15
31	930	485.22

RESISTIVITY SURVEY

FIG. 15: TRAVERSE: NSK / RS5

LOCATION: UNIVERSITY POULTRY ROAD

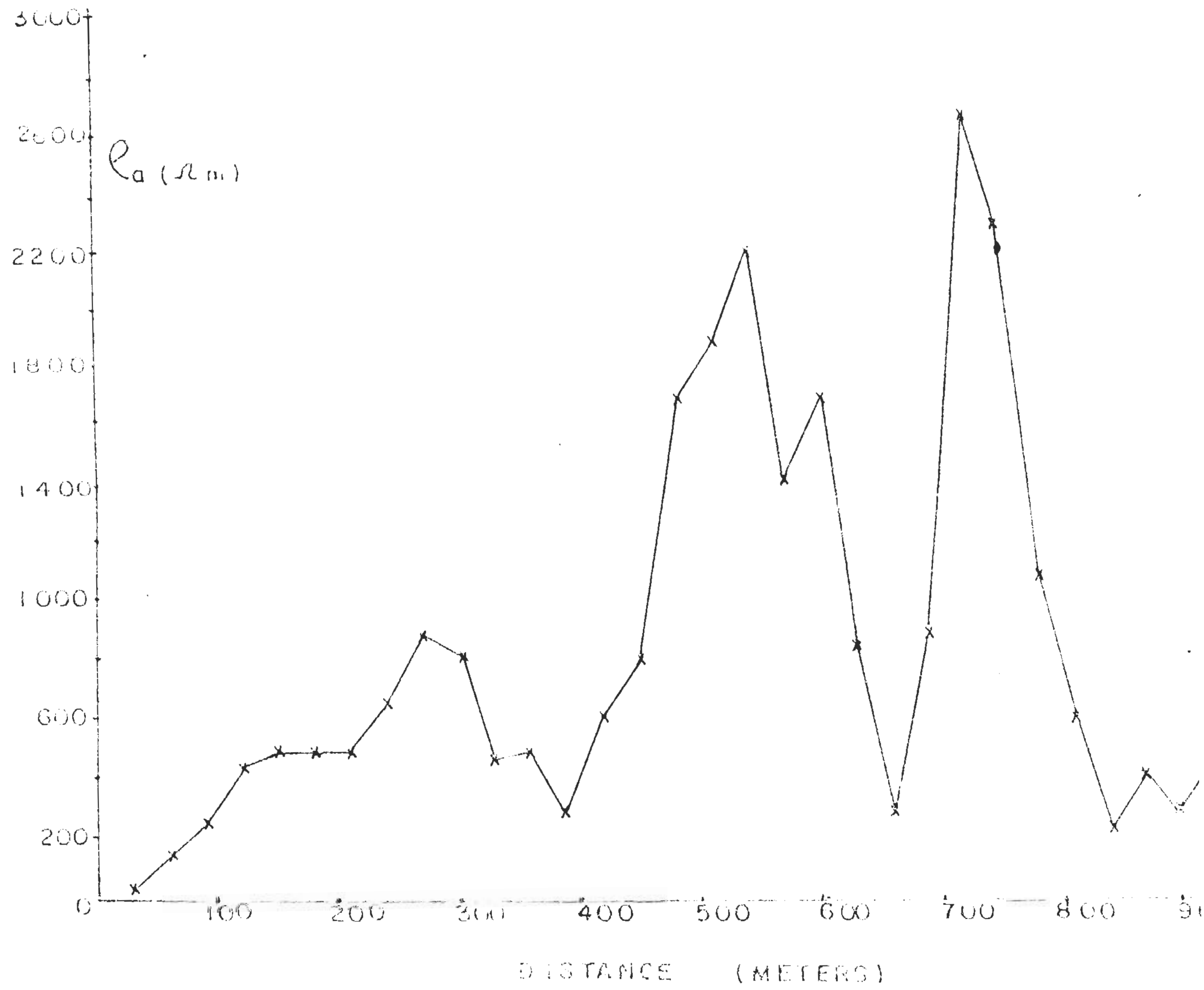

A depth control of 10m's was chosen for the horizontal profiling, only resistivity contrast within that depth can be detected by the equipment. The electrode separation is 10m's apart and this was also used for profiles NSK/RS6 and NSK/RS7 respectively.

From the graph it can be observed that high resistivity values exist between 480m and 600m, and between 720m and 750m respectively with occasionally low resistivity values as well as minor distortions between 30m and 450m, 630m and 690m, 780m and 930m. The high resistivity values show or indicate the presence of low conductive material, for instance, lateritic material that exist within the study area, while the low resistivity values is indicative of high conductive materials, e.g. shale, mud stones that can be seen within the mapped area as well as faulting and fracturing.

6.1.1(f) Profile NSK/RS6

The traverse was carried out at Odenigwe Road, on a bearing of 175^0 Azimuth (refer to fig. 1). The apparent resistivity values were plotted against distances (in meters) see fig. 16 and table 7, and a distance of 930m's was covered.

Resistivity high and low values were observed in the graph between 270m and 300m, 360m and 390m, and then at 450m, 510m respectively for the high values. For the low values between 30m and 180m in an ascending form, 330m, 420m and between 570m to 930m there is also distortions between these distances. The interpretation given here is essentially similar to that given in profile NSK/RS 5.

6.1.1(g) Profile NSK/RS7

The apparent resistivity readings got from the field for NSK/RS7 was plotted against the center spread or distance (in meters) as shown in fig. 17 and table 8. The profile was run along the quarry site at hill top

Table 7 **Resistivity Survey**

Traverse: NSK/RS6

Location: Odenigwe Road

Bearing: 175^0

S/No.	Distance (M)	ϱ_a (Ohm – Meters)
1	30	18.86
2	60	40.73
3	90	118.81
4	120	115.41
5	150	213.09
6	180	356.42
7	210	422.41
8	240	492.31
9	270	626.27
10	300	697.75
11	330	265.52
12	360	610.99
13	390	514.82
14	420	213.85
15	450	551.59

Table 7 Cont.

16	480	425.44
17	510	452.03
18	540	363.21
19	570	214.99
20	600	94.29
21	630	245.53
22	660	228.18
23	690	281.93
24	720	294.18
25	750	165.01
26	780	196.12
27	810	203.67
28	840	184.81
29	870	164.06
30	900	260.24
31	930	233.84

RESISTIVITY SURVEY

FIG.16: TRAVERSE: NSK / RS6

LOCATION: ODENIGWE ROAD

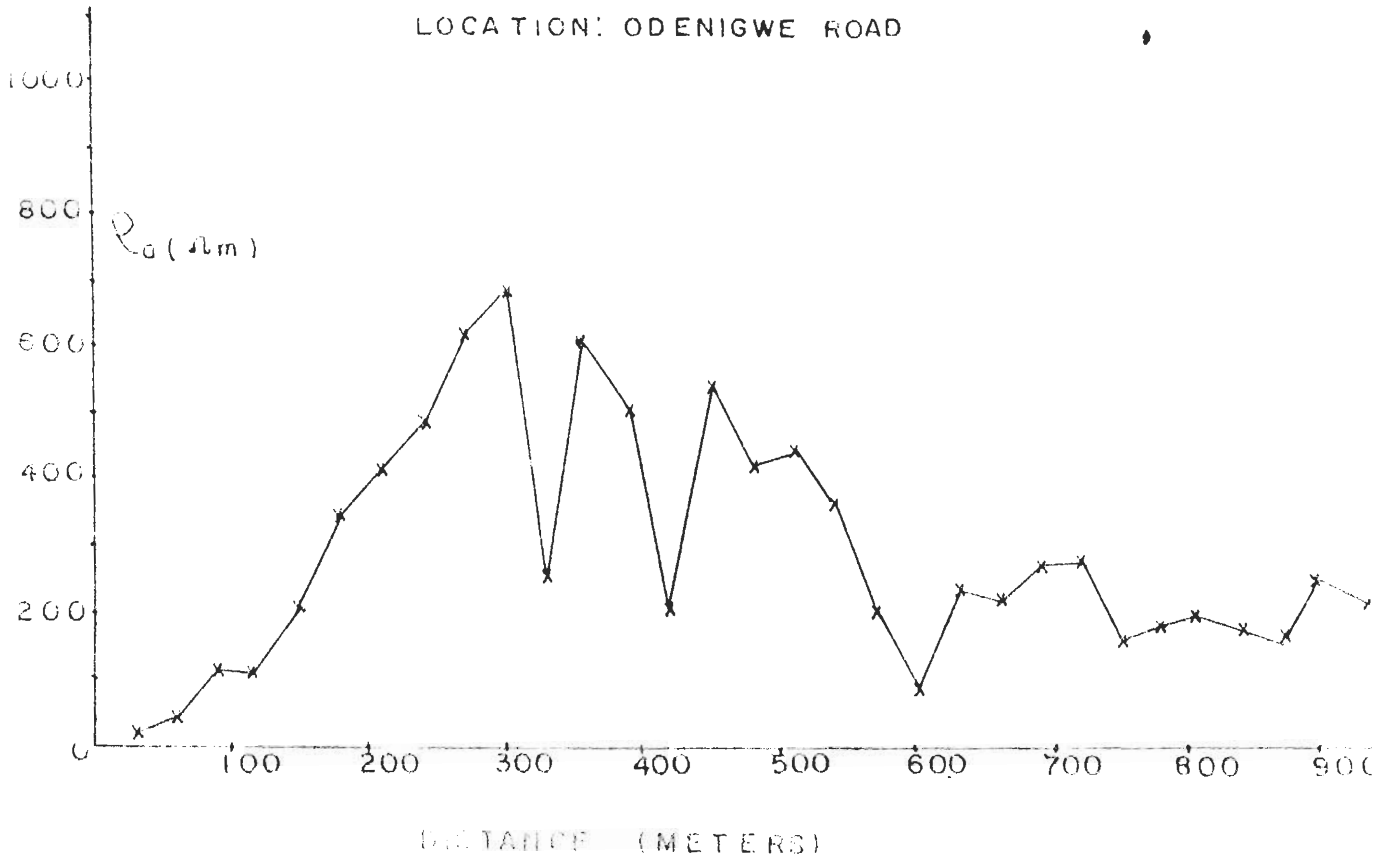

Table 8 **Resistivity Survey**

Traverse: NSK/RS7

Location: Quarry Site at Hill Top U.N.N.

Bearing: 340^0

S/No.	Distance (M)	ϱ_a (Ohm – Meters)
1	30	49.03
2	60	56.57
3	90	87.12
4	120	99.57
5	150	124.46
6	180	113.15
7	210	62.04
8	240	113.15
9	270	96.74
10	300	56.57
11	330	62.23
12	360	131.25
13	390	154.45
14	420	190.09
15	450	260.24

Table 8 Cont.

16	480	75.43
17	510	92.97
18	540	78.07
19	570	136.15
20	600	143.32
21	630	71.28
22	660	124.46
23	690	307.95
24	720	321.34
25	750	141.44
26	780	215.74
27	810	147.66
28	840	132.01
29	870	180.47
30	900	599.68
31	930	315.68

RESISTIVITY SURVEY

FIG. 17: TRAVERSE: NSK/RS7

LOCATION: QUARRY SITE AT HILL TOP UNN

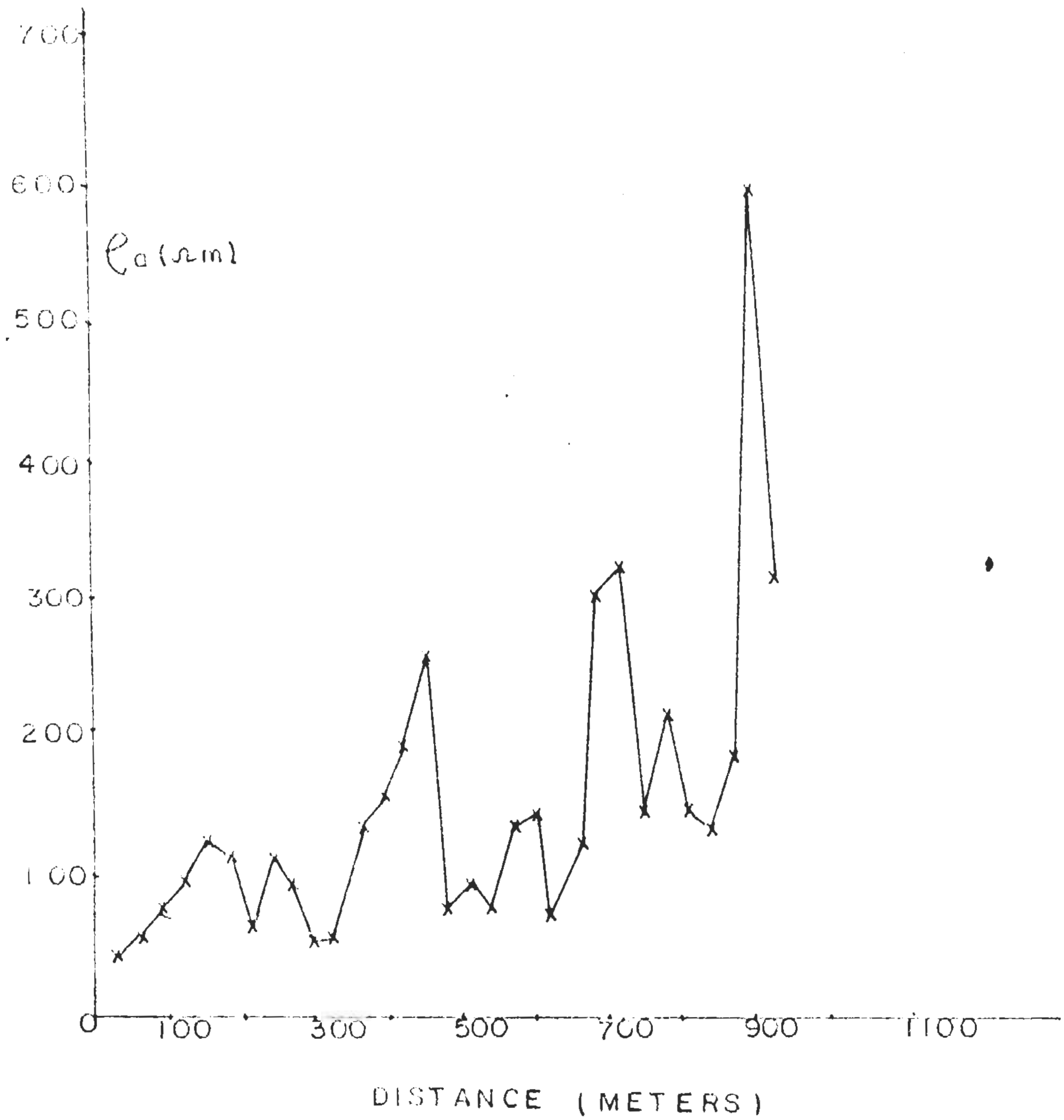

U.N.N at a bearing of 340° Azimuth and a total distance of 930m's was covered (refer to fig. 1).

It could be observed in the profile that low resistivity values and distortions exists between 30m and 330m, between 480m and 660m and between 750m and 870m respectively while high resistivity values exist between 360m and 450m, between 690m, 720m and 900m. The interpretation for this profile is similar to the interpretation given in the previous profiles for high and low resistivity values.

6.1.2 Magnetic Surveys

Magnetic surveys were carried out in the same area where the resistivity measurements were conducted.

Eleven profiles (NSK/Mg 1 – 8 and LEJ/Mg 1 – 3) were obtained. The profiling were taken along the grid line as shown on the base map (refer to base map fig. 1). For all the profiles, a total of 9,760m (9.760km) meters of distance was covered. Some profiles also ran perpendicular. These are NSK/Mg 3 and NSK/Mg 8.

The principle of the method is that wherever there is a change in magnetic coordinates e. g from positive to negative or vice versa, an anomaly is detected by the magnetometer. Hence, one of the most useful applications of magnetic surveys is to map structural trends by following lineation in magnetic contours Dobrin (1976). The lineations may reflect the strike lines of elongated intrusive features or the surfaces of faults reflected in the topography. For this work, the profiles were taken along the grid line as seen on the geologic or base map. Robert (1974) observed however, that the magnetic method is a relatively ineffective tool to detect and delineate faults, this nonetheless, does not necessarily preclude its effectiveness in environments where linear concentrations of magnetite occur along faults.

The survey conducted was not a regional one and it was therefore not necessary to carry out corrections for diurnal, terrain etc.

From the data obtained, graphs of vertical magnetic intensity (ΔZ) in gammas were plotted against the lateral distances in meters as shown in figures 18 – 28.

An attempt to interpret the sections of the eleven profiles NSK/Mg 1 – 8 and LEJ/Mg 1 – 3 revealed that the almost smooth regional could be indicative of a sedimentary environment which does not contain or possess magnetic susceptible materials. An assumed arbitrary datum was determined for each profile and the range was between 5247 gammas and 5259 gammas respectively, the average of all the individual readings.

6.1.2(a) Profile NSK/Mg 1

Figure 18 and table 9 show the profile for NSK/Mg 1. The profile was taken at a bearing of 334^0 and a distance of 1,120 meters was covered. A plot of vertical magnetic intensity (ΔZ) in gammas was plotted against the lateral distance in meters, and an assumed arbitrary datum of 5255 gammas was used.

Table 9 **Magnetic Survey**

Traverse: **NSK/Mg 1**

Location: **Ibeagwa Road**

Bearing: **334^0**

S/No.	Distance (M)	Δ Z (Gammas)
1	0	5265
2	40	5244
3	80	5255
4	120	5244
5	160	5265
6	200	5265
7	240	5255
8	280	5255
9	320	5255
10	360	5255
11	400	5244
12	440	5244
13	480	5233
14	520	5265
15	560	5255

Table 9 Cont.

16	600	5255
17	640	5265
18	680	5244
19	720	5265
20	760	5255
21	800	5265
22	840	5255
23	880	5255
24	920	5255
25	960	5265
26	1000	5255
27	1040	5255
28	1080	5265
29	0	5255

MAGNETIC SURVEY

FIG.18: TRAVERSE: NSK/ Mgl

LOCATION: IBEGWA ROAD

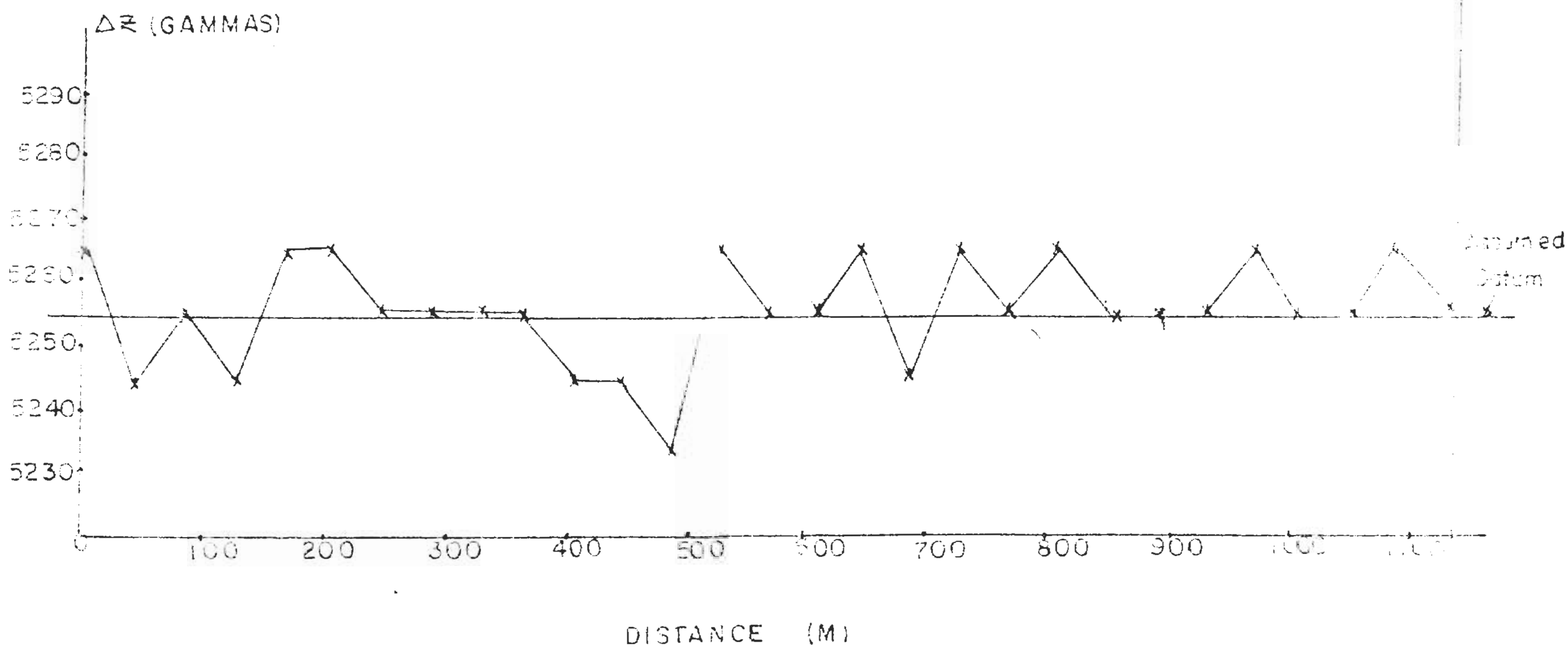

From the profile, it is observed that magnetic low exist between 120m, 400m to 480m and 680m while magnetic highs existed between 160m to 240m, 520m to 840m, 720m to 1120m.

Change in polarity from positive to negative coordinate was observed between 360m, 540m while change in polarity from negative to positive is observed between 120m, 480m, 680m respectively.

Minor distortions exist between the distances of 520m to 840m.

The change in polarity from positive to negative or from negative to positive coordinate is suggestive of probably minor fault or fracture points or even joints. The depression or distortions around 520m to 840m may suggest areas of inherent weakness (fracture or joints).

6.1.2 (b) Profile NSK/Mg 2

Figure 19 and table 10 show the profiles for NSK/Mg 2. The profile was taken at a bearing of 124^0 and a distance of 560m was covered. It should be noted that the magnetic survey was carried out along the line in which the resistivity profiles were done (refer to fig. 1). A plot of vertical magnetic intensity (ΔZ) in gammas against the lateral distance in meters and an assumed arbitrary datum of 5257 gammas is shown in Fig. 19.

From the profile, it is observed that magnetic high exist between 40m, 120m, and 200m, 360m and 400m. Change in polarity was observed from negative to positive between 80m, 240m and 440m, similarly change in polarity from positive to negative was observed between 360m and 120m. Magnetic low exist between 240m and 350m. The changes from either magnetic "low" to magnetic "high" or from magnetic "high" to magnetic "low" is interpreted as suggestive of fault or fracture points or contact between two rock types of different susceptibilities.

Table 10 **Magnetic Survey**

Traverse: **NSK/Mg 2**

Location: **Opposite NSK/Mg 1**

Bearing: **124^0**

S/No.	Distance (M)	Δ Z (Gammas)
1	0	5265
2	40	5276
3	80	5255
4	120	5265
5	160	5265
6	200	5265
7	240	5255
8	280	5244
9	320	5233
10	360	5265
11	400	5265
12	440	5255
13	480	5255
14	520	5244
15	0	5255

MAGNETIC SURVEY

FIG. [illegible] TRAVERSE: NSK/Mg 2

LOCATION: OPPOSITE NSK/Mg 1

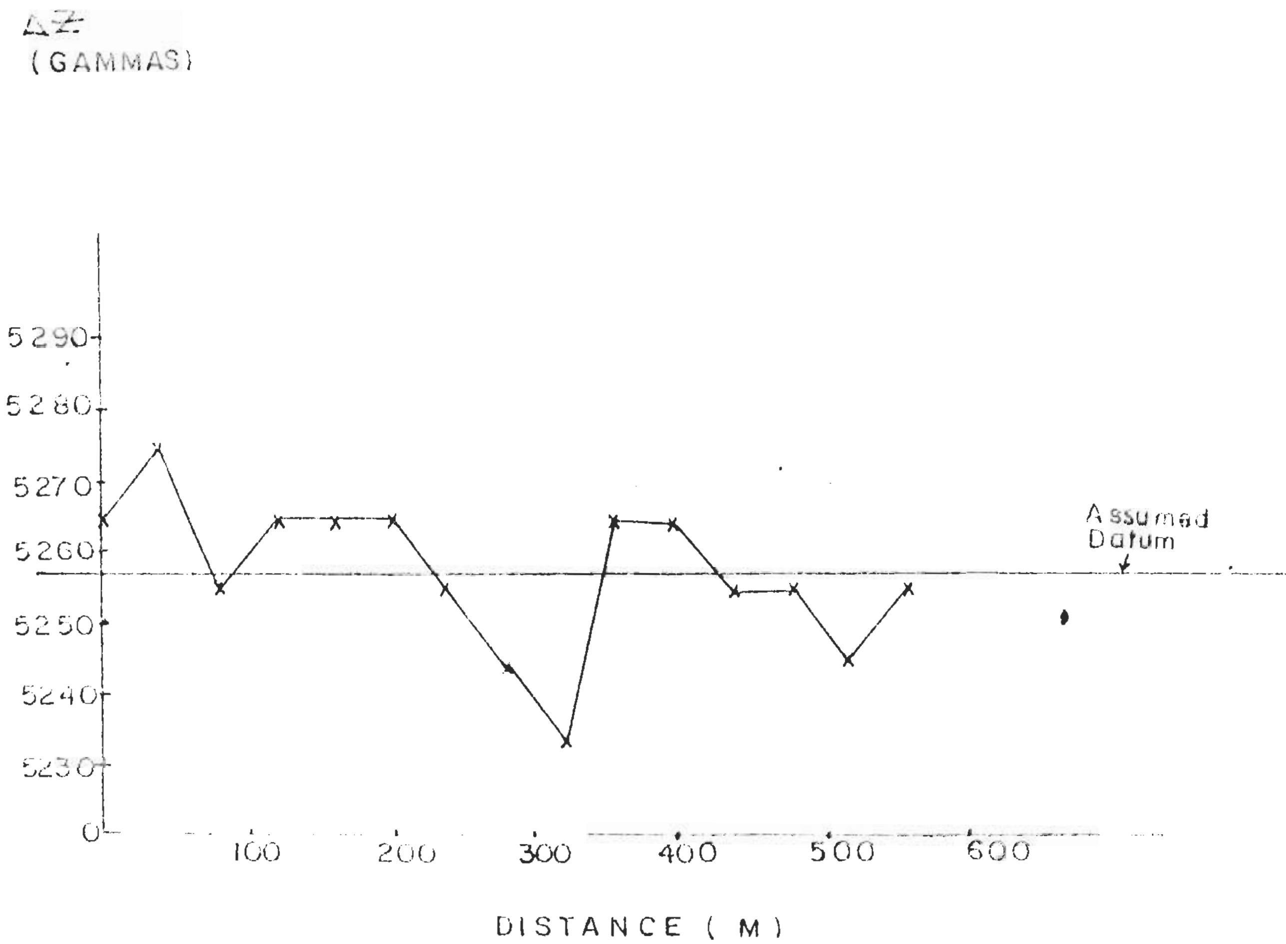

6.1.2(c) Profile NSK/Mg 3

Profile NSK/Mg 3 is shown in figure 20 and table 11. It was taken on a bearing of 55^0 and perpendicular to NSK/Mg2, a distance of 440m was covered. Assumed datum was 5249 gammas.

Magnetic high exist between 40m, 160m and 200m, 360m and 440m while magnetic low exist between 80m and 120m, 240m and 320m, 400m.

Change in polarity from negative to positive occurs at locations 120m, 320m, and 400m, while the change in polarity from positive to negative coordinate was observed between 40m, 200m and 360m.

Essentially, the interpretation given in 6.1.2(b) above is applicable to 6.1.2(c).

6.1.2(d) Profile NSK/Mg 4

Figure 21 and table 12 show the profiles for NSK/Mg4. A distance of 960m was covered on a

Table 11 **Magnetic Survey**

Traverse: **NSK/Mg 3**

Location: **Perpendicular to NSK/Mg 2**

Bearing: **55^0**

S/No.	Distance (M)	Δ Z (Gammas)
1	0	5265
2	40	5265
3	80	5244
4	120	5244
5	160	5255
6	200	5255
7	240	5233
8	280	5244
9	320	5255
10	360	5255
11	400	5244
12	0	5255

MAGNETIC SURVEY

FIG. 20: TRAVERSE NSK/ Mg3

LOCATION: PERPENDICULAR TO NSK/Mg2

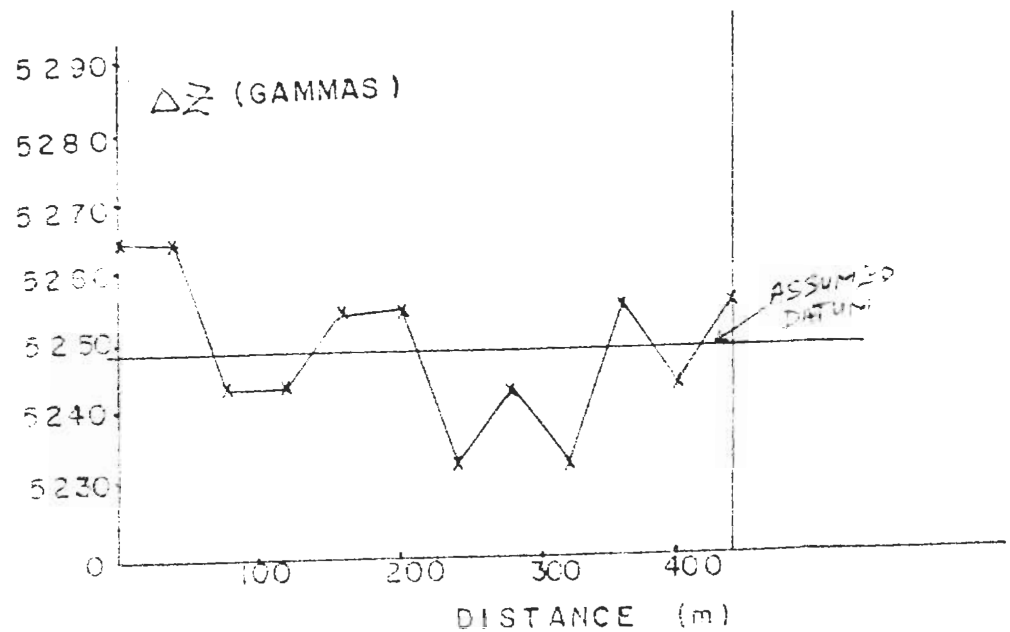

Table 12 **Magnetic Survey**

Traverse: **NSK/Mg 4**

Location: **105m from NSK/Mg 2**

Bearing: **110^0**

S/No.	Distance (M)	Δ Z (Gammas)
1	0	5265
2	40	5255
3	80	5255
4	120	5255
5	160	5244
6	200	5265
7	240	5265
8	280	5265
9	320	5265
10	360	5255
11	400	5255
12	440	5054
13	480	5265
14	520	5265
15	560	5255

Table 12 Cont.

16	600	5244
17	640	5244
18	680	5233
19	720	5244
20	760	5265
21	800	5276
22	840	5255
23	880	5255
24	920	5244
25	0	5255

MAGNETIC SURVEY

FIG. 21: TRAVERSE: NSK/Mg4
LOCATION: 105 METERS FROM NSK/Mg 2

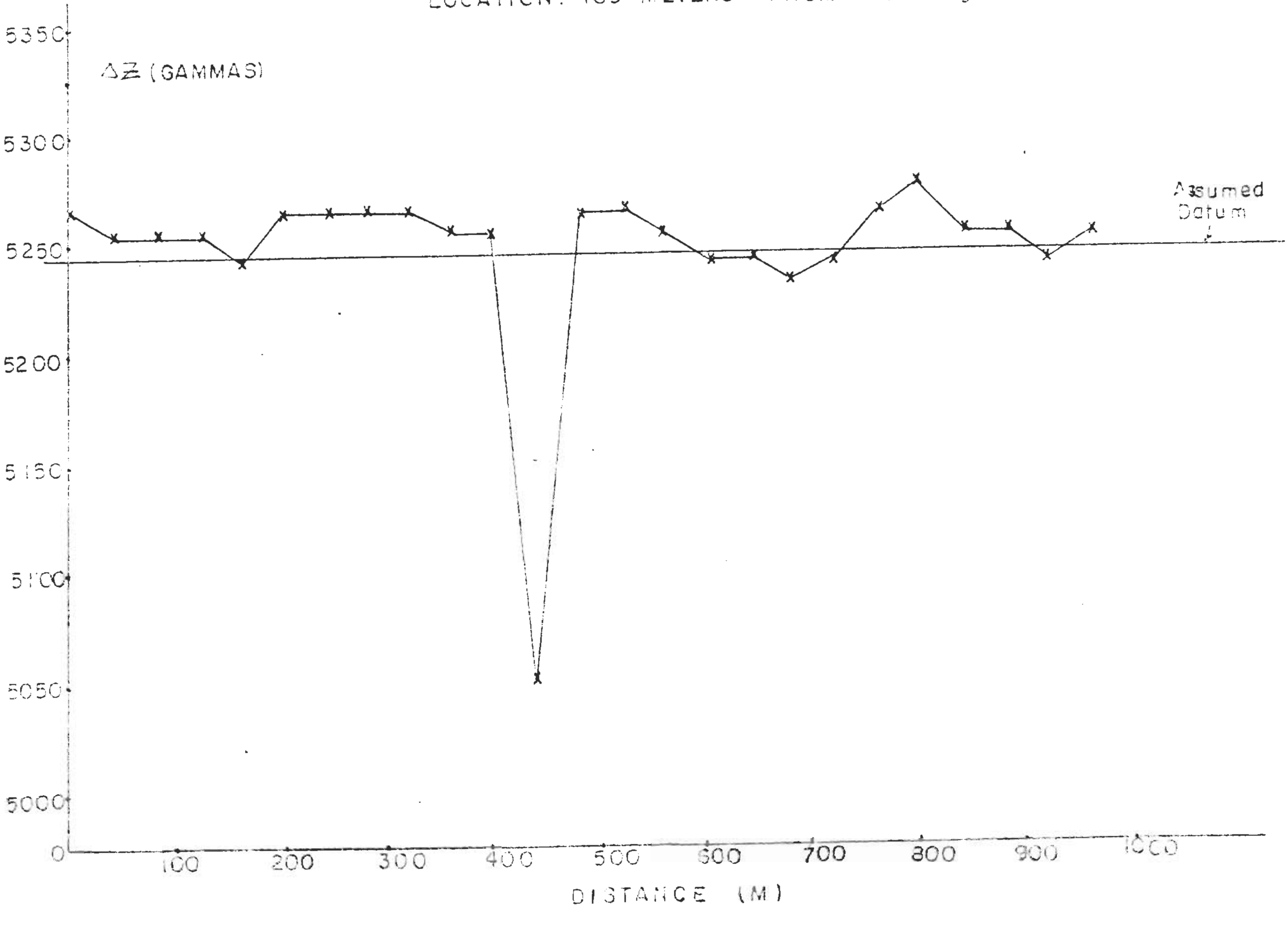

bearing of 110^{o} and an assumed datum of 5247 gammas was used.

Between 40m to 120m, 200m to 400m, 470m to 560m, 760m to 880m and 960m magnetic highs can be observed, change in polarity between positive to negative can be observed between 120m, 400m, 560m, and 880m respectively. While between 160m, 600m and 720m, 920 magnetic lows exist further between 600m and 720 minor distortions can be observed. Change in polarity from negative to positive was observed between 160m, 440m, 720m and 920m respectively.

But worthy of note is the very extensive magnetic low (or anomaly) observed between 400m and 480m, this probably can be interpreted to be the metallic pipe used in channeling sewage from the University community to the central sewage system located within that area.

The interpretation given in 6.1.2 (b) is also applicable to 6.1.2 (d).

6.1.2(e) Profile NSK/Mg5

Figure 22 and table 13 show the profiles for NSK/Mg5. A total distance of 1040 meters was covered for this profile on a bearing of 139^0. An assumed datum of 5255 gammas was derived.

Magnetic high were observed at the following distances 200m to 280m, 640m, 760m to 920m and 1040 while magnetic lows existed between 80m, 400m to 560m, 720m, 960m to 1000m.

Change in polarity from positive to negative was observed between 40m, 280m, 680m, 920m and change in polarity from negative to positive is from 160m, 600m, 720m, 1000m respectively.

The change in polarity from positive to negative or from negative to positive coordinate suggest minor fault or fracture or joint set, or contacts between two rock types of different susceptibilities.

Table 13 **Magnetic Survey**

Traverse: **NSK/Mg 5**

Location: **University Poultry Road**

Bearing: **139^0**

S/No.	Distance (M)	Δ Z (Gammas)
1	0	5265
2	40	5255
3	80	5244
4	120	5255
5	160	5255
6	200	5265
7	240	5265
8	280	5265
9	320	5255
10	360	5255
11	400	5255
12	440	5244
13	480	5233
14	520	5244
15	560	5255

Table 13 Cont.

16	600	5255
17	640	5265
18	680	5255
19	720	5244
20	760	5265
21	800	5265
22	840	5265
23	880	5276
24	920	5265
25	960	5244
26	1000	5233
27	0	5265

MAGNETIC SURVEY

FIG. 22: TRAVERSE: NSK, Mg8

LOCATION: UNIVERSITY POULTARY ROAD

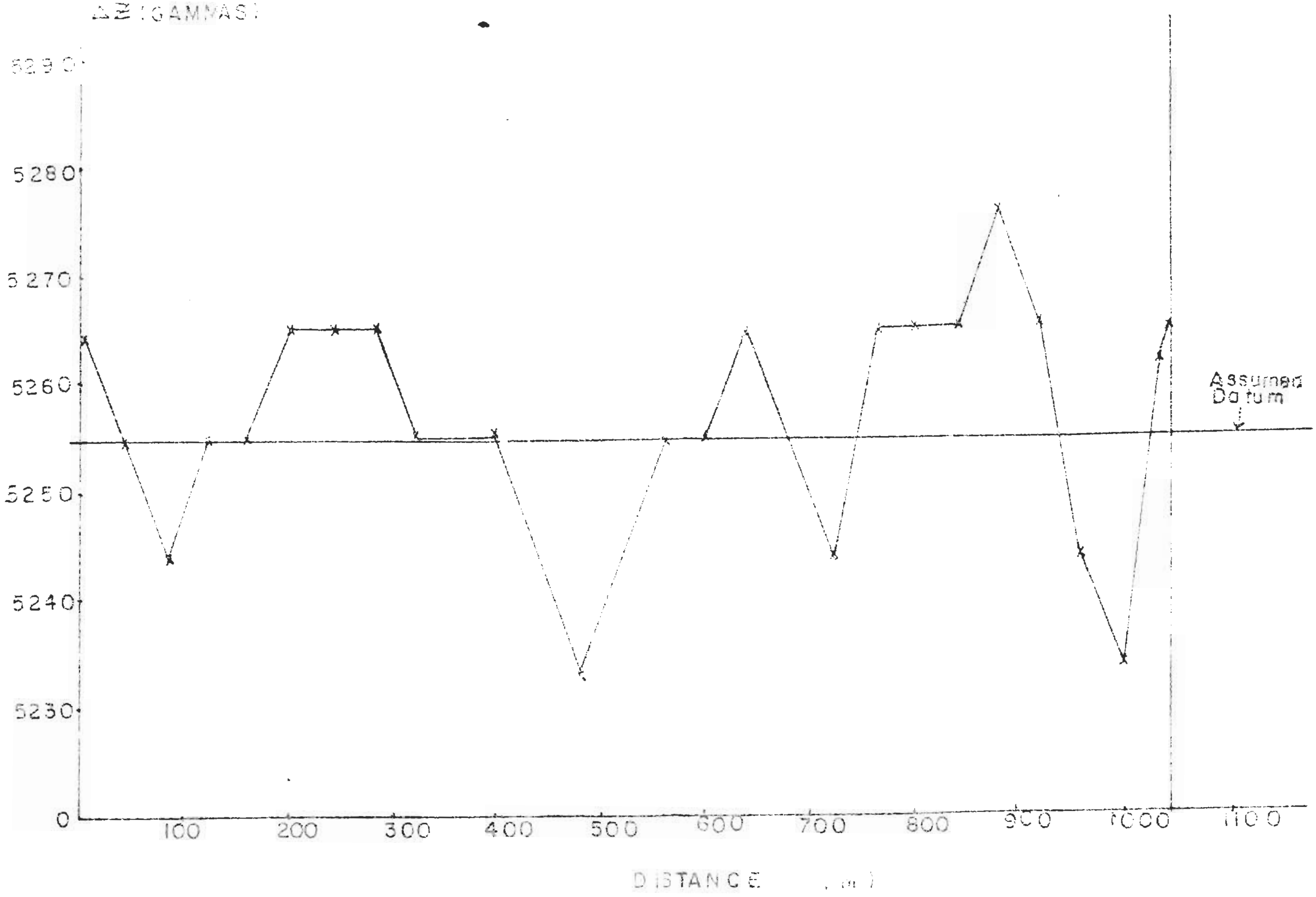

6.1.2(f) Profile NSK/Mg6

Profile NSK/Mg6 is shown in figure 23 and table 14. This was taken on a bearing of 175^0 along Odenigwe Road, Nsukka, a distance of 1040m was covered (refer to fig. 1). A plot of vertical magnetic intensity (ΔZ) in gammas was plotted against lateral distance in meters, assumed datum of 5253 gammas is given.

Between 40m to 80m, 160m, 240m to 320m, 400m to 520m, 600m, 720m, 840m and 1000m magnetic high is observed. Change in polarity from positive to negative was observed at 80m, 160m, 320m, 520m, 640m, 720m and 870 while between 120m, 200m, 360m, 560m, 680m, 760m to 800m and 920m to 960m magnetic low was observed. Change in polarity from negative to positive was observed between 120m, 200m, 360m, 560m, 680m, 800m and 960m respectively.

The interpretation given in 6.1.2 (b) above is applicable to 6.1.2 (f).

Table 14 **Magnetic Survey**

Traverse: NSK/Mg 6

Location: Odenigwe Road, Nsukka

Bearing: 175^0

S/No.	Distance (M)	ΔZ (Gammas)
1	0	5265
2	40	5265
3	80	5255
4	120	5244
5	160	5265
6	200	5244
7	240	5255
8	280	5255
9	320	5276
10	360	5244
11	400	5255
12	440	5255
13	480	5255
14	520	5265
15	560	5244

Table 14 Cont.

16	600	5255
17	640	5255
18	680	5244
19	720	5255
20	760	5244
21	800	5244
22	840	5255
23	880	5255
24	920	5244
25	960	5244
26	1000	5255
27	0	5255

MAGNETIC SURVEY

FIG. 23: TRAVERSE: NSK/ Mg 6

LOCATION: ODENIGWE ROAD

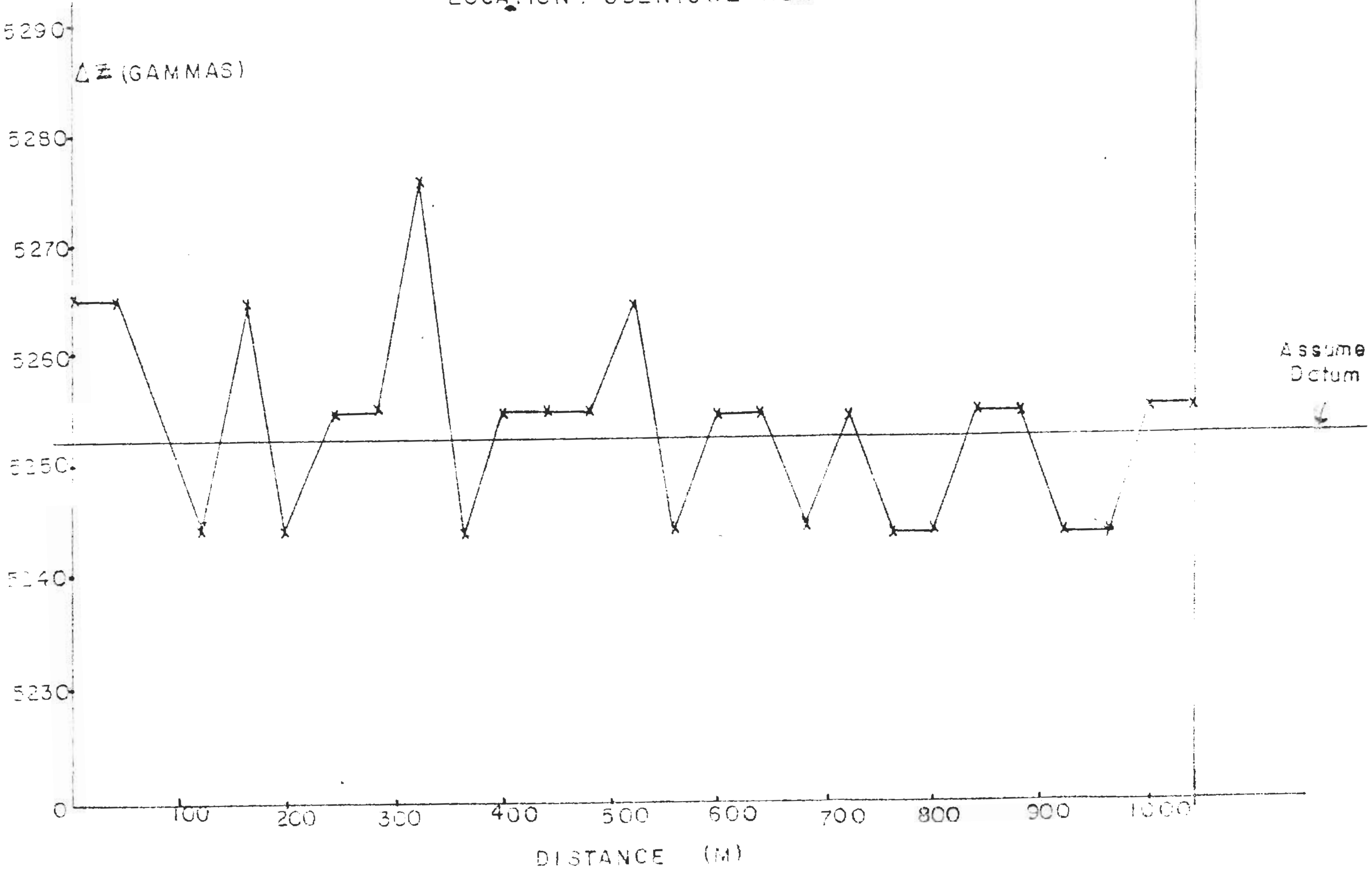

6.1.2(g) Profile NSK/Mg 7

Figure 24 and table 15 represents profile NSK/Mg 7. It was taken on a bearing of 340^0 and a distance of 920m was covered. The traversing or profiling was performed at a discarded quarry site at hilltop U.N.N. A plot of vertical magnetic intensity (ΔZ) in gammas versus distance in meters was plotted, an assumed datum of 5251 gammas is given.

Magnetic high was observed between 40m to 120m, 240m to 320m, 400m, 470m to 640m and 920 while magnetic low was observed between 160m to 200m, 360m to 440m and between 680m to 880m.

Change in polarity from positive to negative was observed at 120m, 320m, 640m while change in polarity from negative to positive was observed at 200m, 360m, 440m and 880m respectively.

The interpretation of the profile is similar to the interpretation of the previous profiles.

Table 15 Magnetic Survey

Traverse: **NSK/Mg 7**

Location: **Quarry Site at Hill Top U.N.N.**

Bearing: **340^{0}**

S/No.	Distance (M)	Δ Z (Gammas)
1	0	5265
2	40	5255
3	80	5265
4	120	5265
5	160	5244
6	200	5244
7	240	5255
8	280	5265
9	320	5265
10	360	5244
11	400	5255
12	440	5233
13	480	5276
14	520	5255
15	560	5255

Table 15 Cont.

16	600	5255
17	640	5255
18	680	5244
19	720	5244
20	760	5233
21	800	5244
22	840	5233
23	880	5233
24	0	5255

MAGNETIC SURVEY

FIG. 24: TRAVERSE: NSK / Mg 7

LOCATION: QUARRY SITE AT HILL TOP UNN

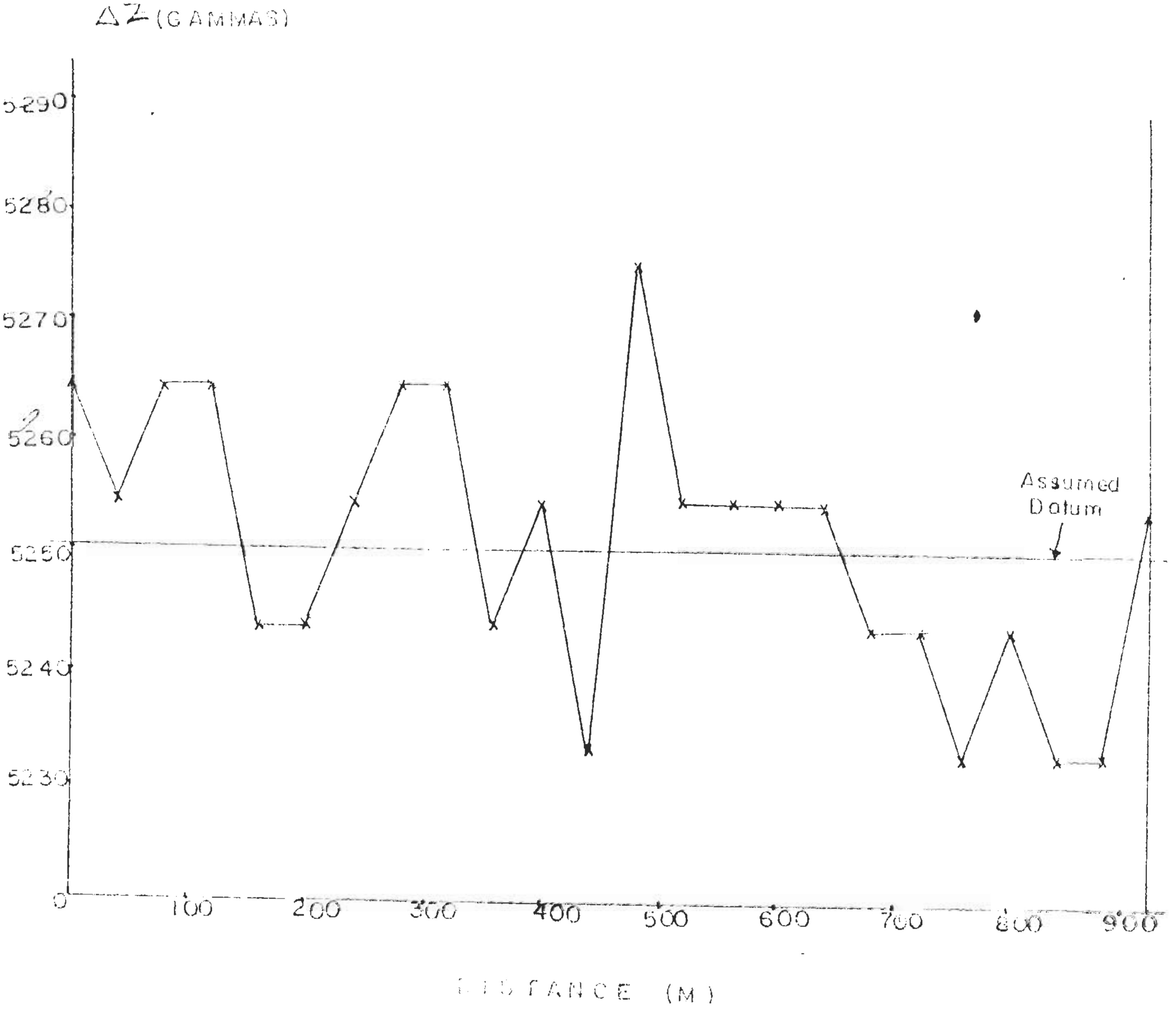

6.1.2(h) Profile NSK/Mg 8

Figure 25 and table 16 show the profile for NSK/Mg 8. The profile was taken perpendicular to NSK/Mg7 on a bearing of 265^0. A distance of 560m was taken and a plot of vertical magnetic intensity (ΔZ) in gammas versus distance in meters was plotted. Assumed datum is 5259 gammas.

Magnetic high was observed between 40m to 80m 200m, 320m, and 440m to 480m. Change in polarity from positive to negative was observed between 80m, 200m, 320m and 480m while magnetic low was observed at 120m to 160m, 240m to 280m, 360m to 400m and 520m to 560m respectively.

The interpretation of the magnetic high to low as well as change in polarity from positive to negative or negative to positive coordinates is suggestive of probably minor faults, fracture or joints.

Table 16 Magnetic Survey

Traverse: NSK/Mg 8

Location: Perpendicular To NSK/Mg 7

Bearing: 265^0

S/No.	Distance (M)	Δ Z (Gammas)
1	0	5265
2	40	5265
3	80	5276
4	120	5255
5	160	5255
6	200	5265
7	240	5244
8	280	5244
9	320	5265
10	360	5255
11	400	5255
12	440	5265
13	480	5276
14	520	5255
15	0	5255

MAGNETIC SURVEY

FIG.25: TRAVERSE: NSK/Mg8

LOCATION: PERPENDICULAR TO NSK/Mg7

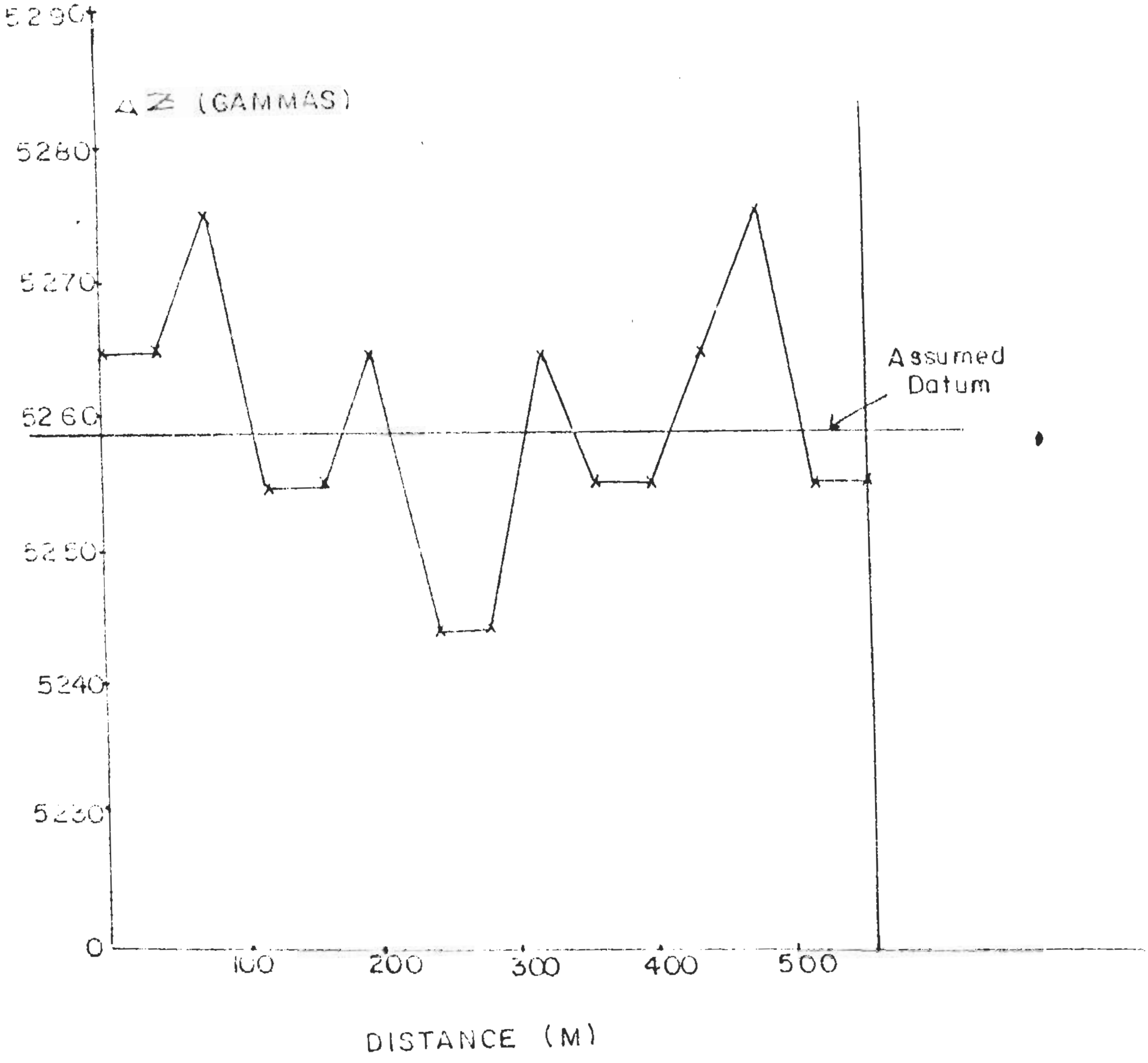

6.1.2(i) Profile LEJ/Mg 1

Figure 26 and table 17 show the profile LEJ/Mg 1. The profile was taken at Lejja area. A total distance of 1040 was covered on a bearing of 340^0. The vertical magnetic intensity value in gammas was plotted against distance in meters, the assumed datum is 5258 gammas.

Magnetic highs were observed at, between 40m to 640m, 800m to 920m while the magnetic low lie between 40m to 400m, 680m to 760m, 960m to 1040m.

Change in polarity from positive to negative coordinate was observed at 640m and 920m while change in polarity from negative to positive was observed at 400m and 760m respectively.

The interpretation for this profile suggests that the changes in polarity from positive to negative and vice versa could probably indicate minor fault or fracture point or contact between two rock types of different susceptibilities.

Table 17 **Magnetic Survey**

Traverse: **LEJ/Mg 1**

Location: **Lejja**

Bearing: **340^0**

S/No.	Distance (M)	Δ Z (Gammas)
1	0	5265
2	40	5255
3	80	5255
4	120	5244
5	160	5255
6	200	5244
7	240	5244
8	280	5233
9	320	5255
10	360	5244
11	400	5244
12	440	5265
13	480	5265
14	520	5275
15	560	5265

Table 17 Cont.

16	600	5275
17	640	5286
18	680	5255
19	720	5244
20	760	5244
21	800	5286
22	840	5286
23	880	5265
24	920	5275
25	960	5255
26	1000	5255
27	0	5255

MAGNETIC SURVEY

FIG. 26 TRAVERSE: LEJ/ Mgl

LOCATION: LEJJA

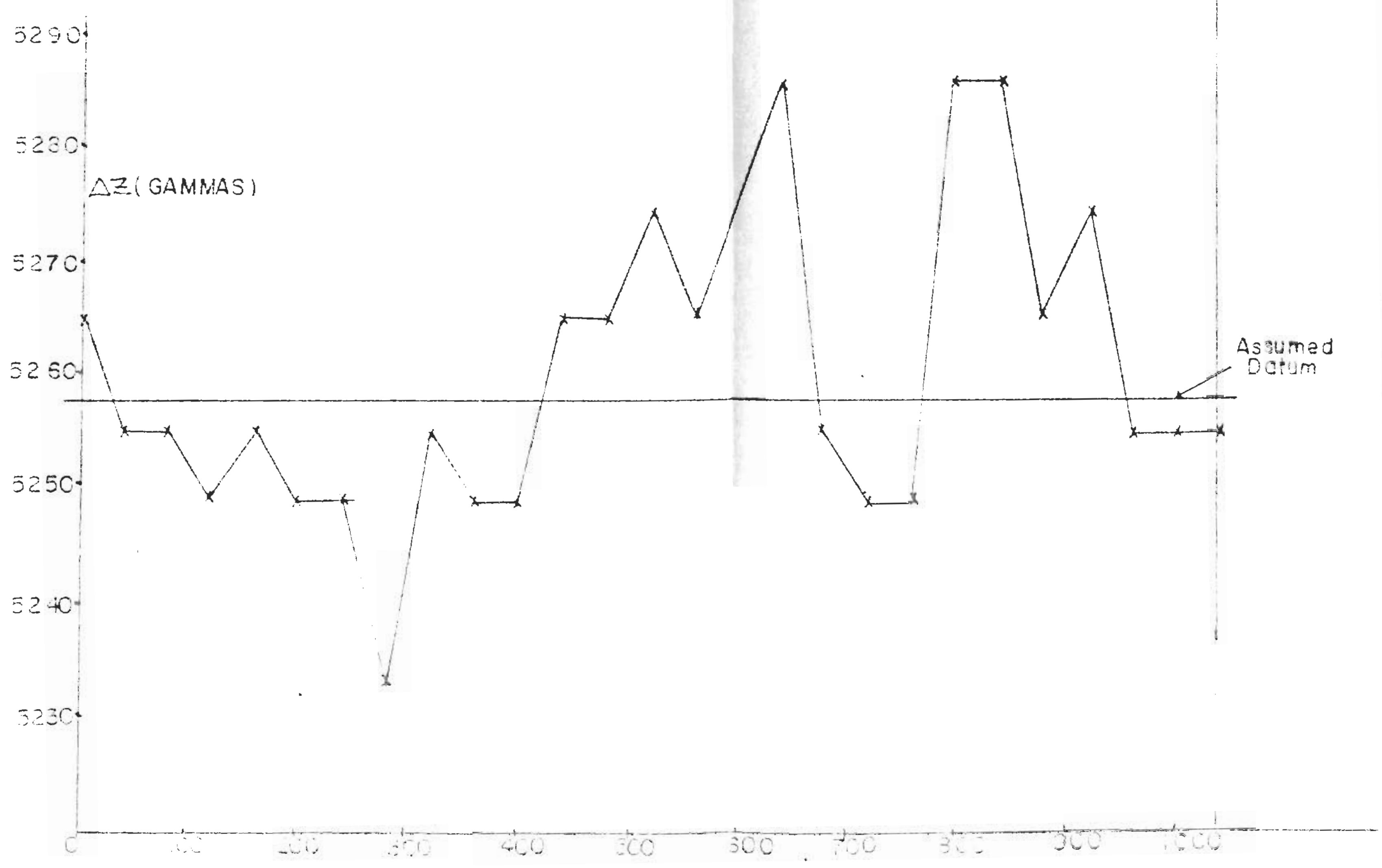

6.1.2(j) Profile LEJ/Mg 2

Figure 27 and Table 18 show the profile LEJ/Mg2. The profile distance is 1040m and on a bearing of 345^0. The vertical magnetic intensity value (ΔZ) in gammas was plotted against lateral distance in meters. The assumed datum is 5255 gammas.

From the profile magnetic highs were observed at 480m to 760m and between 960m to 1040m while magnetic low were observed at 40m to 440m and 800m to 920m.

Change in polarity from positive to negative coordinate were observed at 40m, 760m while vice versa. It was observed at 440m and 920m.

The interpretation for the previous profile 6.1.2 (i) is applicable to this profile 6.1.2 (j).

6.1.2(k) Profile LEJ/Mg 3

Profile LEJ/Mg 3 is shown in figure 28 and table 19. It was taken on a bearing of 160^0 and a distance of

Table 18 **Magnetic Survey**

Traverse: **LEJ/Mg 2**

Location: **Lejja**

Bearing: **345^0**

S/No.	Distance (M)	Δ Z (Gammas)
1	0	5265
2	40	5255
3	80	5244
4	120	5233
5	160	5233
6	200	5244
7	240	5244
8	280	5244
9	320	5255
10	360	5255
11	400	5255
12	440	5244
13	480	5265
14	520	5275
15	560	5275

Table 18 Cont.

16	600	5286
17	640	5286
18	680	5265
19	720	5265
20	760	5255
21	800	5244
22	840	5244
23	880	5233
24	920	5233
25	960	5275
26	1000	5265
27	0	5265

MAGNETIC SURVEY

FIG. 27: TRAVERSE: LEJ/Mg 2

LOCATION: LEJJA

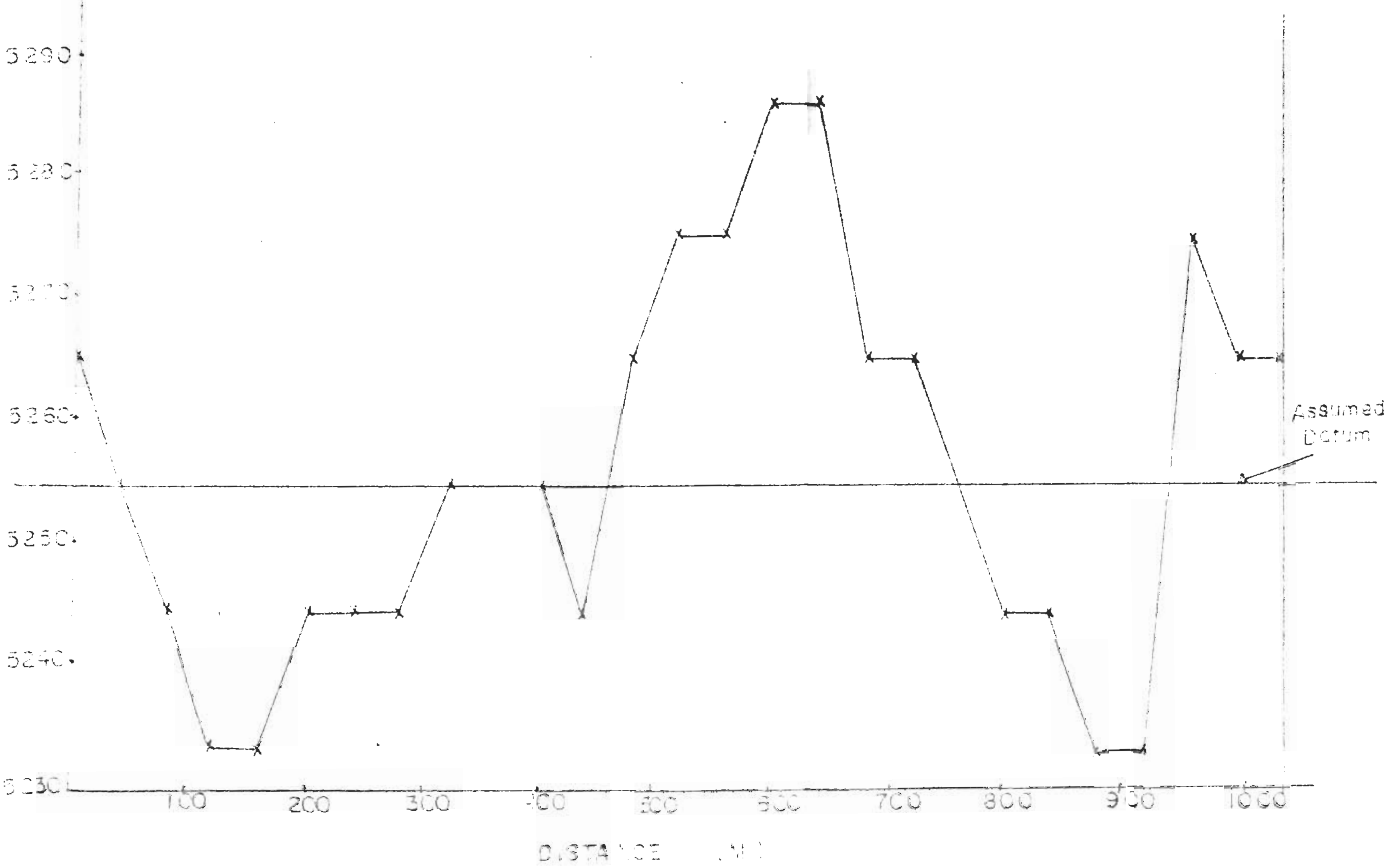

Table 19 **Magnetic Survey**

Traverse: **LEJ/Mg 3**

Location: **Lejja**

Bearing: **160^0**

S/No.	Distance (M)	Δ Z (Gammas)
1	0	5265
2	40	5265
3	80	5265
4	120	5255
5	160	5244
6	200	5233
7	240	5233
8	280	5244
9	320	5265
10	360	5265
11	400	5255
12	440	5255
13	480	5244
14	520	5233
15	560	5244

Table 19 Cont.

16	600	5255
17	640	5244
18	680	5244
19	720	5233
20	760	5233
21	800	5244
22	840	5265
23	880	5275
24	920	5275
25	960	5286
26	1000	5265
27	0	5265

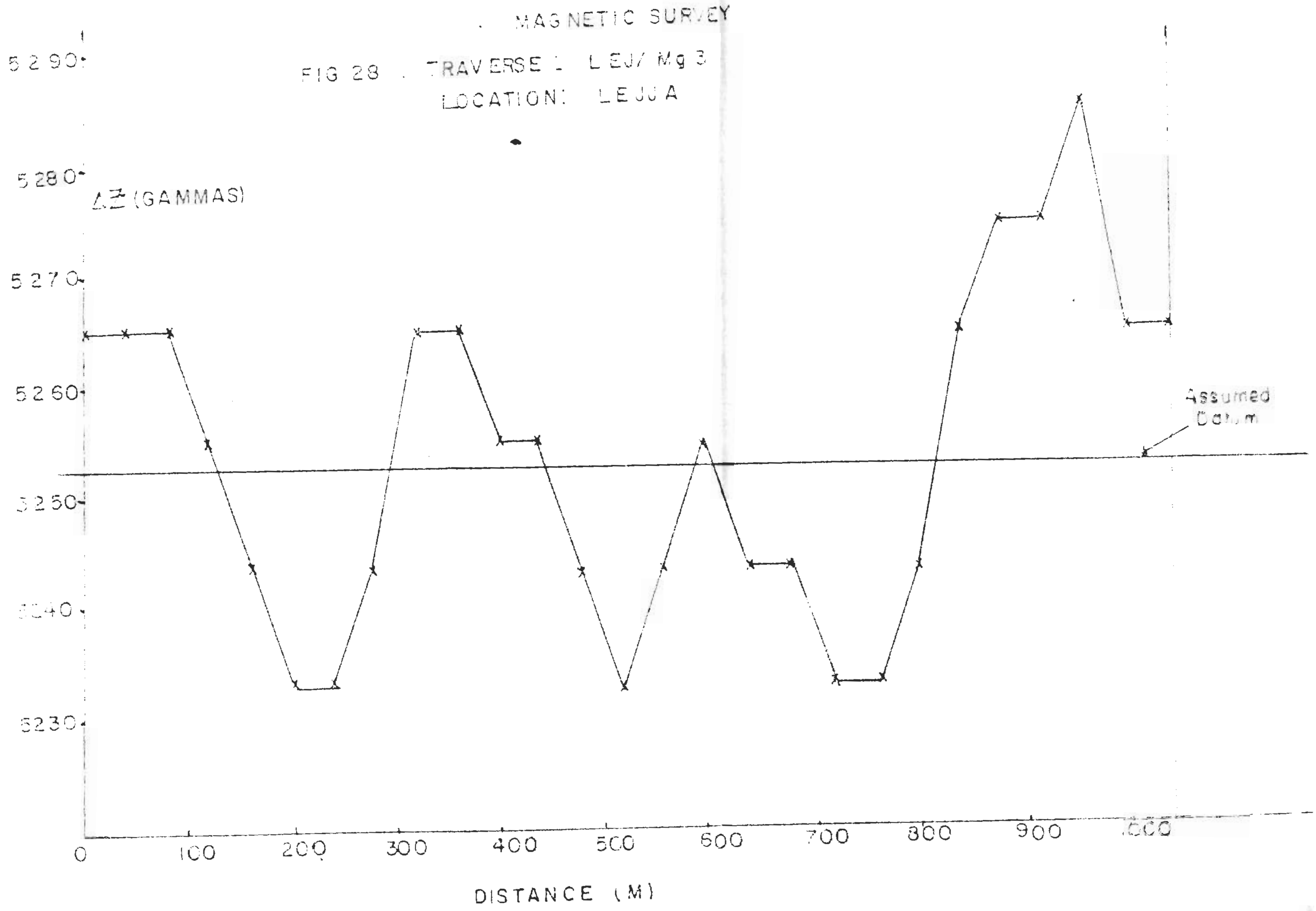
MAGNETIC SURVEY
FIG 28 . TRAVERSE 1 LEJ/ Mg 3
LOCATION: LEJJA
5290
5280
ΔZ (GAMMAS)
5270
5260
5250
5240
5230
Assumed Datum
0
100
200
300
400
500
600
700
800
900
1000
DISTANCE (M)

1040 covered. A plot of vertical magnetic intensity (ΔZ) in gammas versus lateral distance in meters was plotted, and an assumed datum of 5253 gammas given.

From the profile change in polarity from positive to negative coordinate was observed between 120m, 440m, 600m, while change in polarity from negative to positive is between 280m, 560m and 800m respectively.

Magnetic high were observed between 40m to 120m, 320m to 440m, 600m, 840m to 1040 while magnetic low were observed at 160m to 280m, 480m to 560m and 640m to 800m respectively.

CHAPTER SEVEN

DISCUSSION

Results of the resistivity interpretation and magnetic surveys, like those of many other types of geological or geophysical investigation, are interpreted by comparison with a catalog of reference surveys for different geologic situations. Further, we can employ the use of anomaly index diagrams, as is the case with only electromagnetic (Em) surveys (Strangway 1969, Joshi et al., 1984 in Mamah and Eze 1988).

Seven resistivity profiles were carried out and a total of 4,725 meters (4.725km) were covered. The apparent resistivity in ohm-meters were plotted against center spread (distance) in meters and the profiles (fig. 11 – 17) interpreted. The profiles show resistivity highs and low with some distances showing minor distortions. Roberts (1973) observed that since any subsurface discontinuity within the range of resistivity equipment may cause variations in the resistivity, it is important to consider the variations that are likely to be caused by faults in the earths crust. Further, it is important to note the principles of this method of resistivity profiling which is that an anomaly which indicates a fault or fracture is indicated by an abrupt contrast in resistivity values got along the traverse line, Dobrin (1976). From the foregoing, the intermittent resistivity high and low along the traverse line show or suggest faulting, fracturing, joint sets, or primarily suggests differences in rock types or geology of the area. The general trend taken for the profiling is in a NW – SE direction.

The magnetic survey was taken along the grid line (refer to figure 1a & b) on an aeromagnetic map 287, Nsukka sheet of 1965. It should be noted that the magnetic survey was taken along the same line in which the resistivity surveys were carried out, in effect the resistivity profile served as a complimentary survey for the magnetic survey and/or vice versa. The principles of the magnetic method are that wherever there is a change in magnetic property, an anomaly is detected by the magnetometer, Dobrin (1976). From the profiles (fig. 18 – 28) magnetic highs and low were observed as well as changes in polarity from positive to negative and/or from negative to positive. These changes indicate or suggest minor faults, fracture or joints, or even contacts between two rock types of different susceptibilities.

A total distance of 9,769 meters (9.760km) was covered, assumed datum was determined by averaging each profile reading. The trend of the profiling is in a NW – SE direction.

Within point A in the aeromagnetic map, we observe close magnetic contours while the topographic map equally shows close contour with high contour values. This area is the quarry site at hill top U.N.N. Ground magnetic survey conducted within this area revealed no visible anomaly, this probably indicates that susceptible magnetic minerals within this area are either inexistent or have been completely quarried (refer to figure 24, 25 and table 15, 16). Within point B in the aeromagnetic map, we observe an open but elongated magnetic contour stretching towards the western section of the map while the topographic map though show no closure, but rather high contour values can be observed. Ground magnetic surveys carried out within this area revealed slight variations (refer to figure 26, 27, 28 and table 17, 18, 19).

Generally, cross-sections were drawn for the geologic map figure 1(a) and aeromagnetic map figure 1(b) (A – B and C – B) to reflect their contours. The aeromagnetic map contours were of total magnetic field intensity in gammas. It was observed that the geologic map showed gradual increase in contour value with dome shape (see cross-section for A – B and C – B, geologic map). While the aeromagnetic map showed flat but linearly increasing shape, suggesting the presence of susceptible magnetic material. At the beginning of the cross-section (C - B) for the aeromagnetic map slight increase in form was observed suggesting probably presence of susceptible magnetic materials while towards the centre depression, suggesting absence of magnetic susceptible material and at the end increase in form was observed too. (see cross-section for A – B and C – B, aeromagnetic map).

7.1 STATISTICAL ANALYSIS FOR THE RESISTIVITY AND MAGNETIC VALUES

7.1.1 Cross Correlation Analysis

Cross correlation deals with the comparison of two time series. We perform cross correlation in order to determine the position of complete equivalence between the two time series.

The equation for cross correlation is the same as that of the ordinary linear correlation coefficient. If we designate the two series as Y_1 and Y_2 and define n as the number of overlapping positions, the cross correlation coefficient for match position m is given as:

$$R_m = \frac{n\Sigma Y_1 Y_2 - \Sigma Y_1 Y_2}{\sqrt{[n\Sigma Y_1^2 - (\Sigma Y_1)^2]\,[n\Sigma Y_2^2 - (\Sigma Y_2)^2]}}$$

Davis, (1973).

Interpretation of Cross Correlation

The cross correlation coefficient ranges from −1 to +1, and is a measure of the degree of linear association of the two time series. If the coefficient is equal to +1, Y_1 and Y_2 are said to be perfectly directly or positively correlated; if the coefficient is equal to −1, Y_1 and Y_2 are said to be perfectly inversely or negatively correlated; if it is zero, Y_1 and Y_2 are said to be uncorrelated, though this does not mean that they might not be associated in some way other than linearly.

7.1.2 Test of Significance of Cross Correlation Coefficient

To test the significance of a cross correlation coefficient, r_m we calculate

$$t = r_m \sqrt{\frac{n-2}{1-r_m^2}}$$

Davis, (1973)

And locate the values of t in the t-distribution table (table 20), for the appropriate value of (n – 2) degrees of freedom. The null hypothesis is that the correlation between apparent resistivity and that of the magnetic reading is zero. This hypothesis is to be tested on the assumption that it is true. The value of p corresponding to t as given by the table is the probability that a value of r_m could arise from random sampling of the variables, Y_1 and Y_2, Brookes (1953).

It is customary before starting any experiment on correlation to select some critical probability. Therefore null hypothesis (H_0) states that r_m is equal to 0 and the alternative hypothesis (H_1) states that r_m is not equal to 0, at an α level of significance 5% & 1%.

i.e. H_0: $r_m = 0$

H_1: $r_m \neq 0$

α = 5% & 1%

Percentile Values (t_p) for Student's t Distribution with ν Degrees of Freedom

TABLE 20

ν	$t_{.55}$	$t_{.60}$	$t_{.70}$	$t_{.75}$	$t_{.80}$	$t_{.90}$	$t_{.95}$	$t_{.975}$	$t_{.99}$	$t_{.995}$
1	.158	.325	.727	1.000	1.376	3.08	6.31	12.71	31.82	63.66
2	.142	.289	.617	.816	1.061	1.89	2.92	4.30	6.96	9.92
3	.137	.277	.584	.765	.978	1.64	2.35	3.18	4.54	5.84
4	.134	.271	.569	.741	.941	1.53	2.13	2.78	3.75	4.60
5	.132	.267	.559	.727	.920	1.48	2.02	2.57	3.36	4.03
6	.131	.265	.553	.718	.906	1.44	1.94	2.45	3.14	3.71
7	.130	.263	.549	.711	.896	1.42	1.90	2.36	3.00	3.50
8	.130	.262	.546	.706	.889	1.40	1.86	2.31	2.90	3.36
9	.129	.261	.543	.703	.883	1.38	1.83	2.26	2.82	3.25
10	.129	.260	.542	.700	.879	1.37	1.81	2.23	2.76	3.17
11	.129	.260	.540	.697	.876	1.36	1.80	2.20	2.72	3.11
12	.128	.259	.539	.695	.873	1.36	1.78	2.18	2.68	3.06
13	.128	.259	.538	.694	.870	1.35	1.77	2.16	2.65	3.01
14	.128	.258	.537	.692	.868	1.34	1.76	2.14	2.62	2.98
15	.128	.258	.536	.691	.866	1.34	1.75	2.13	2.60	2.95
16	.128	.258	.535	.690	.865	1.34	1.75	2.12	2.58	2.92
17	.128	.257	.534	.689	.863	1.33	1.74	2.11	2.57	2.90
18	.127	.257	.534	.688	.862	1.33	1.73	2.10	2.55	2.88
19	.127	.257	.533	.688	.861	1.33	1.73	2.09	2.54	2.86
20	.127	.257	.533	.687	.860	1.32	1.72	2.09	2.53	2.84
21	.127	.257	.532	.686	.859	1.32	1.72	2.08	2.52	2.83
22	.127	.256	.532	.686	.858	1.32	1.72	2.07	2.51	2.82
23	.127	.256	.532	.685	.858	1.32	1.71	2.07	2.50	2.81
24	.127	.256	.531	.685	.857	1.32	1.71	2.06	2.49	2.80
25	.127	.256	.531	.684	.856	1.32	1.71	2.06	2.48	2.79
26	.127	.256	.531	.684	.856	1.32	1.71	2.06	2.48	2.78
27	.127	.256	.531	.684	.855	1.31	1.70	2.05	2.47	2.77
28	.127	.256	.530	.683	.855	1.31	1.70	2.05	2.47	2.76
29	.127	.256	.530	.683	.854	1.31	1.70	2.04	2.46	2.76
30	.127	.256	.530	.683	.854	1.31	1.70	2.04	2.46	2.75
40	.126	.255	.529	.681	.851	1.30	1.68	2.02	2.42	2.70
60	.126	.254	.527	.679	.848	1.30	1.67	2.00	2.39	2.66
120	.126	.254	.526	.677	.845	1.29	1.66	1.98	2.36	2.62
∞	.126	.253	.524	.674	.842	1.28	1.645	1.96	2.33	2.58

Source: R. A. Fisher and F. Yates, *Statistical Tables for Biological, Agricultural and Medical Research*, published by Longman Group Ltd., London (previously published by Oliver and Boyd, Edinburgh), and by permission of the authors and publishers.

Decision rule: States that we reject H_0 if t_{cal} is greater than t_{tab}, otherwise we accept.

If p is greater than 5%, the null hypothesis is accepted; if p is between 5% and 1%, the null hypothesis is rejected with reasonable confidence; if p is less than 1%, the null hypothesis is confidently rejected, Brookes, (1953).

7.2(a) Comparison for NSK/RS1 and NSK/Mg1

The apparent resistivities obtained were correlated with the magnetic reading for NSK/RS1 and NSK/Mg1, the first twenty nine (29) variables were taken from each way. The mean and standard deviation for each profile gave 5255.45 and 8.4159 for the magnetic profile, while 276.28 and 148.712 for the resistivity profile. The correlation coefficient was given as –0.213 and the test of significance show that t has a value of –1.132 for 27 degrees of freedom. This shows that the absolute value of t_{cal} (-1.132) is less than t_{tab} (2.0518), therefore we accept H_0 and conclude that correlation coefficient is not statistically significant or that null hypothesis is true. P is between 0.10 and 0.20.

7.2(b) *Comparison for NSK/RS2 and NSK/Mg2*

The apparent resistivities obtained were correlated with the magnetic reading for NSK/RS2 and NSK/Mg2, the first fifteen (15) variables were taken from each way. The mean and standard deviation for magnetic and resistivity values is 5257.47; 10.94 and 166.75; 118.85 respectively. Correlation coefficient is –0.267 and t is –0.999 for 13 degrees of freedom. This implies that the absolute value of t_{cal} (-0.999) is less than t_{tab} (2.1604), we accept H_0 and conclude that the correlation coefficient is not statistically significant or that null hypothesis is true. P is between 0.10 and 0.20.

7.2(c) *Comparison for NSK/RS3 and NSK/Mg3*

The apparent resistivities obtained were correlated with the magnetic values for NSK/RS3 and NSK/Mg3, the first twelve (12) variables were taken from each way. The mean and standard deviation for magnetic and resistivity profiles are 5251.167; 9.495 and 295.088; 175.496 respectively. The correlation coefficient was given as –0.375 and t is –1.2795 for 10 degrees of freedom. This implies that the absolute value of t_{cal} (-1.2795) is less than t_{tab} (2.2281), therefore we accept H_0 and conclude that the correlation coefficient is not statistically significant or that null hypothesis is true. P is between 0.10 and 0.20.

7.2(d) Comparison for NSK/RS4 and NSK/reMg4

Apparent resistivity values were correlated with the magnetic values for NSK/RS4 and NSK/Mg4, the first twenty-five (25) variables were taken from each way. The mean and the standard deviation for each profile gave 5247.92 and 41.572 for the magnetic profile while 718.3312 and 470.152 for resistivity profile.

The correlation coefficient was given as –0.019 and test of significance show that t has a value of –0.091 for 23 degrees of freedom. This implies that the absolute value of t_{cal} (-0.091) is less than t_{tab} (2.0687), therefore we accept H_0 and conclude that the correlation coefficient is not statistically significant or that null hypothesis is true. P is between 0.10 and 0.20.

7.2(e) Comparison for NSK/RS5 and NSK/Mg5

Apparent resistivity values were equally correlated with the magnetic values for NSK/RS5 and NSK/Mg5, the first twenty-seven (27) variables were taken from each way. The mean and standard deviation for magnetic and resistivity values is 5255.44; 10.577 and 920.145; 662.52 respectively.

Correlation coefficient is 0.0585 and t is 0.293 for 25 degrees of freedom since the absolute value of t_{cal} (0.293) is less than t_{tab} (2.0595), it calls for an acceptance of H_0 and we conclude that there is no significant difference, or that the null hypothesis is true. P is between 0.30 and 0.40.

7.2(f) Comparison for NSK/RS6 and NSK/Mg6

The two profiles were correlated NSK/RS6 and NSK/Mg6 and the first twenty-seven (27) variables were taken from each way. The mean and standard deviation for the magnetic and resistivity profiles is given as 5253; 8.4955 and 311.978; 185.08 respectively.

The correlation coefficient is given as –0.045 and t is –0.225 for 25 degrees of freedom. P is between 0.40 and 0.45

This implies that since the absolute value of t_{cal} (-0.225) is less than t_{tab} (2.0595), we accept H_0 and conclude that the correlation coefficient is not statistically significant or that null hypothesis is true.

7.2(g) Comparison for NSK/RS and NSK/Mg7

Two profiles were correlated NSK/RS7 and NSK/Mg7 and the first twenty-four (24) variables were taken from each way. The mean and standard deviation for the magnetic and resistivity profiles is given as 5251.54; 12.007 and 125.318; 75.379 respectively.

The correlation coefficient is given as –0.18394 and t is –0.877 for 22 degrees of freedom. P is between 0.10 and 0.20. This shows that since the absolute value of t_{cal} (-0.877) is less than t_{tab} (2.0739) we accept H_0 and conclude that the correlation coefficient is not statistically significant or that the null hypothesis is true.

A programme called S.P.S.S. version 7.5 was used to find the segments of the apparent resistivity and magnetic readings that gave the best correlation, it was observed that the results of the software matched the results obtain by arithmetic/statistical calculations (see table 21 to 24) for only the correlation coefficient (r_m). Other parameters were derived by using their various formulas.

TABLE 21

Correlations for NSK/RS1 & NSK/Mg1

Descriptive Statistics

	Mean	Std. Deviation	N
GAMM_MG1	5255.4483	8.4159	29
OHM_RS1	276.2845	148.7117	29

Correlations

		GAMM_MG1	OHM_RS1
Pearson Correlation	GAMM_MG1	1.000	-.177
	OHM_RS1	-.177	1.000
Sig. (2-tailed)	GAMM_MG1	.	.359
	OHM_RS1	.359	.
N	GAMM_MG1	29	29
	OHM_RS1	29	29

Correlations for NSK/RS2 & NSK/Mg2

Descriptive Statistics

	Mean	Std. Deviation	N
GAMM_MG2	5257.4667	10.9405	15
OHM_RS2	166.7487	118.8489	15

Correlations

		GAMM_MG2	OHM_RS2
Pearson Correlation	GAMM_MG2	1.000	-.267
	OHM_RS2	-.267	1.000
Sig. (2-tailed)	GAMM_MG2	.	.336
	OHM_RS2	.336	.
N	GAMM_MG2	15	15
	OHM_RS2	15	15

TABLE 22

Correlations for NSK/RS3 & NSK/Mg3

Descriptive Statistics

	Mean	Std. Deviation	N
GAMM_MG3	5251.1667	9.4948	12
OHM_RS3	295.0883	175.4958	12

Correlations

		GAMM_MG3	OHM_RS3
Pearson Correlation	GAMM_MG3	1.000	-.375
	OHM_RS3	-.375	1.000
Sig. (2-tailed)	GAMM_MG3	.	.230
	OHM_RS3	.230	.
N	GAMM_MG3	12	12
	OHM_RS3	12	12

Correlations for NSK/RS4 & NSK/Mg4

Descriptive Statistics

	Mean	Std. Deviation	N
GAMM_MG4	5247.9200	41.5721	25
OHM_RS4	717.5312	470.9300	25

Correlations

		GAMM_MG4	OHM_RS4
Pearson Correlation	GAMM_MG4	1.000	-.020
	OHM_RS4	-.020	1.000
Sig. (2-tailed)	GAMM_MG4	.	.925
	OHM_RS4	.925	.
N	GAMM_MG4	25	25
	OHM_RS4	25	25

TABLE 23

Correlations for NSK/RS5 & NSK/Mg5

Descriptive Statistics

	Mean	Std. Deviation	N
GAMM_MG5	5255.8148	10.7347	27
OHM_RS5	920.2559	662.5151	27

Correlations

		GAMM_MG5	OHM_RS5
Pearson Correlation	GAMM_MG5	1.000	.112
	OHM_RS5	.112	1.000
Sig. (2-tailed)	GAMM_MG5	.	.577
	OHM_RS5	.577	.
N	GAMM_MG5	27	27
	OHM_RS5	27	27

Correlations for NSK/RS6 & NSK/Mg6

Descriptive Statistics

	Mean	Std. Deviation	N
GAMM_MG6	5253.5926	8.4955	27
OHM_RS6	311.9781	185.0766	27

Correlations

		GAMM_MG6	OHM_RS6
Pearson Correlation	GAMM_MG6	1.000	-.045
	OHM_RS6	-.045	1.000
Sig. (2-tailed)	GAMM_MG6	.	.823
	OHM_RS6	.823	.
N	GAMM_MG6	27	27
	OHM_RS6	27	27

TABLE 24

Correlations for NSK/RS7 & NSK/Mg7

Descriptive Statistics

	Mean	Std Deviation	N
GAMM_MG7	5251.5417	12.0072	24
OHM_RS7	125.3179	75.3786	24

Correlations

		GAMM_MG7	OHM_RS7
Pearson Correlation	GAMM_MG7	1.000	-.184
	OHM_RS7	-.184	1.000
Sig. (2-tailed)	GAMM_MG7	.	.390
	OHM_RS7	.390	.
N	GAMM_MG7	24	24
	OHM_RS7	24	24

CHAPTER EIGHT

SUMMARY AND CONCLUSION

The combination of resistivity profiling and magnetic surveys has proved a good pair for the study of fault or facture points. It is equally noted from the study that horizontal resistivity profiling and magnetic methods can only at best determine the location of faults but cannot determine fault displacement or identify wall rock or Formations flanking a concealed fault. This method of geophysical resistivity and magnetic profiling is of prime importance in detecting and delineating faults and may be considered a reconnaissance tool to indicate areas where more intensive geophysical work might be useful. Further, they are minor subsurface lineament associated with fault zones which are often picked during profiling as minor continuous anomaly or distortions.

Resistivity profiling has helped in the intensive demarcation of the geologic boundary which is usually difficult when done with only geologic survey. The resistivity profiles have established that the Nsukka Formation was generally highly resistive, thus poorly conducting because of the tortuous path of current flow in the surfacial lateritic rock cover of the Nsukka Formation and ferruginized sandstones overlying the Ajali sandstone. While the magnetic survey have revealed that the magnetic 'high' and 'low' and vice versa is suggestive of fault, fracture or contact between two rock types of different susceptibilities.

Worthy of note is that the magnetic survey was done for vertical magnetic intensity and not total magnetic intensity. Furthermore, the survey area is close to magnetic equator and the earth field might be near horizontal. Appreciable vertical field measurement may not be obtained making geological conclusion very difficult.

Susceptibility of sedimentary rocks to magnetic changes are relatively small, compared to that of an igneous rock below the sediment, we may expect low magnetic relief in a sedimentary rock environment. In sedimentary regions especially where the basement depths is roughly between 5000ft – 10,000ft, the magnetic contours are normally smooth and the variations quite small. Here the magnetic anomalies are reflections of the basement rocks rather than near-surface features. Also the larger anomalies are usually caused by susceptibility variations rather than topographic relief in the basement Telford (1978).

The statistical comparison showed that the two variables magnetic and resistivities were uncorrelated for most profiles, their t_{cal} were less than their t_{tab} calling for an acceptance of H_0. Most of the profiles showed no statistical significance and their p values revealed that they were greater than 5%.

REFERENCES

Agagu, O.K., et al (1985) Stratigraphy and Sedimentation in the Senonian Anambra Basin of Eastern Nigeria. Nigerian J. Min Geol., V. 22, pp. 25 – 33.

Ananaba, S.E. (1989). Preliminary Interpretation of the two Gravity Profiles over the Schist Belt of Northwestern Nigeria. Nig. Jour. Min. Geol. Vol. 25; No. 1 and 2, pp. 43 – 50.

Banerjee, I., (1979). Ajalli Sandstone of Crossbedded Sequence; An example from the Ajali Sandstone (Maastrichtian) of Nigeria, Jor. Geol. Min. and Met. Soc. Of India. Vol. 51, No. 2, pp. 67.

Brookes, B.C.,(1953). Introduction to Statistical Method, Heinemann, London.

Burke, K.C., Dessauvagie, T.F.J., and Whiteman, A.J., (1970). The Geological History of the Benue Valley and Adjacent Areas: In African Geology, Dessauvagie (ed.) Ibadan Univ. Press. pp.101 – 107.

Burke, K., et al.,(1971). Opening of the Gulf of Guinea and Geological History of the Benue Depression and Niger Delta. Natural Phys. Sci., V. 233, pp. 51 – 55.

Burke K., et al.,(1973). An Implicatoins of Continental Drift to the Earth Sciences (edit by Tarling, D.H. and Runcorn, S.K.) 727 (Academic Press, London).

Cratchley, C.R and Jones, G.P., (1965). An Interpretation of the Geology and Gravity Anomalies of the Benue Valley, Nigeria; Overseas Geol. Survey, Geophys. Paper No. 1, 26 pp.

Davis, W.C., (1973). Statistics and Data Analysis in Geology, John Wiley and Sons, Inc. New York.

De Swardt, A.M.J., and Casey, O.P., (1961). The Coal Resources of Nigeria. Geol. Surv. Nigeria Bull; 28:100.

Dobrin, M.B., (1976). Introduction to Geophysical Prospecting; 3rd ed., McGraw-Hill Inc. 630p.

Dobrin, M.B., and Savit, G.H., (1988). Introduction to Geophysical Prospecting, McGraw Hill Books Company, London, 4th edition, pp. 250 – 770.

Domzalski, W., (1958). Importance of Aeromagnetics in Evolution of Structural Control of Mineralization. Geophysical Prosp. 6, 1 – 10.

Egboka, B.C.E., (1983). Analysis of the Groundwater Resources of Nsukka Area and Environs, Anambra State, Nigeria. Nig. J. Min., Geol. 20 (1 & 2); 1 – 16.

Grant, N.K.,(1971). The South Atlantic, Benue Trough and Gulf of Guinea Cretaceous Triple Junction; Geol. Soc. America Bull, V. 82, pp. 2295 – 2298.

Grove, A.T., (1951). Land Use and Soil Conservation in Parts of Onitsha Province. Geol. Surv. Rec. pp. 44 – 58.

Hoffman, D., et al.,(1974) Aulacogens and their Genetic Relation to Geosynclines, with a Proterozoic Example from Great Slave Lake Canada. In Modern and Ancient Geosynclinal Sedimentation (ed. R.H. Dott Jr., and R.H. Shaver) pp. 38 – 55. S.E.P.M. Special Publ. No. 19.

Hoque, M., (1971). Petrographic Differentiation of Tectonically Controlled Cretaceous Sedimentary Cycles, Southeastern Nigeria Sed. Geology 17: 225 – 245.

Hoque, M., and Ezepue, M.C., (1977). Petrology and Paleogeography of the Ajali Sandstone. Journ. of Min. Geol., v. 14 (1), pp. 16 – 22.

Hoque, M., and Nwajide, C.S., (1984). Tectono – Sedimentological Evolution of an Elongate Intracratonic Basin (Aulacogen), the Case of Benue Trough of Nigeria, Nig. Jour. Min. Geol. Vol. 21, pp. 1 – 2.

Hoque, M., and Nwajide, C.S., (1984). Tectono-Sedimentological Evolution of an Elongate Intracratonic Basin (Anlacogen). The Case of Benue Trough of Nigeria. Nig. Min. Jour. Geol. V. 21, pp. 19 – 26.

Igbozurike, M.U., (1975). Vegetation Types. In Ofomata, G.E.K. (ed.), Nigeria in Maps, Eastern States-Ethiope Publishing House, Benin City, pp. 30 – 31.

Inyang, P.E.B. (1975). Climate Regions. In Ofomata, G.E.K. (ed). Nigeria in Maps: Eastern States. Ethiope Publishing House, Benin, Nigeria.

Keary, P., and Brooks, M., (1984). An Introduction to Geophysical Exploration, E.L.B.S. – Blackwell Scientific Publications, pp. 517 – 519.

Lapido, K.O.,(1986). Tidal Shelf Depositional Model for the Ajali Sandstone, Anambra Basin, Southwestern

Nigeria. Journ. of African Earth Sciences. Vol. 5, pp. 177 – 185.

Mamah, L.I. and Eze, L.C., (1988). Electromagnetic and Ground Magnetic Survey Over Zones of Lead-Zinc Mineralization in Wanakom (Cross River State), Journal of African Earth Science, Vol. 7, No. 5/6, pp. 749 – 758.

Mamah, L.I. and Ekine, A.S. (1989). Electrical Resistivity of Anisotropy and Tectonism of Basal Nsukka Formation. Nig. Jour. Min. Geol. Vol. 25; No. 1 and 2, pp. 31 – 37.

Mbuk, I.N., et al (1985). The Upper Cretaceous Paleocene Boundary in the Ohafia-Ozu Abam Area, Imo State, Nigeria. Nig. Journ. Geol. Vol. 17, pp. 105 – 112.

Murat, R.C. (1972). Stratigraphy and Paleogeography of the Cretaceous and Lower Tertiary in Southern Nigeria. In Dessauvagie, T.F.J. and Whiteman A.J. (ed) African Geology Univ. Press. Ibadan, pp. 251 – 266.

Nwachukwu, S.O. (1972). The Tectonic Evolution of Southern Portion of the Benue Trough, Unpublished Ph.D. Thesis, Univ. of Nigeria, Nsukka.

Ofoegbu, C.O. (1984). A Model for the Tectonic Evolution of the Benue Trough of Nigeira. Sonderdruck aus dev. Geol. Rundschau. 73 (3) 1007 – 1 –18 Stuttgart.

Ofomata, G.E.K. (1974). Geomorphology of the Enugu-Okigwe Cresta. In Ofomata, G.E.K. (ed), Nigeria in Maps Eastern States. Ethiope Publishing House, Benin, Nigeria, pp. 35 – 37.

Olade, M.A. (1975). Evolution of Nigeria's Benue Trough (Aulacogen). A Tectonic Model Geol. Mag. V. 112, pp. 575 – 583.

Ozoko, D.C. (1988). The Hydrogeology of Nsukka Area and Environs. Anambra State, Nigeria. Unpublished M.Sc. Thesis, University of Nigeria, Nsukka.

Parasnis, D.S., (1962). Principles of Applied Geophysics John Willy and Sons, New York.

Petters, S.W. (1978). Stratigraphic Evolution of the Benue Trough and its Implications for the Upper Cretaceous Paleogeography of W. Africa. Jour. Geol. V. 86. pg. 311 – 322.

Popoff, M., et al. (1986). The Upper Cretaceous Gongila and Pindiga Formations Northern Nigeria. Subdivisions age, Stratigraphic Correlations and Paleogeographic

Implications Euogae geol. Helv. Vol-99. pp. 343 – 363.

Reyment, R.A. (1965). Aspects of the Geology of Nigeria, Ibadan University Press, Nigeria.

Reyment, R.A. and Trait, E.A. (1983). Resumé of the Geology of Nigeria. Lexique Stratigraphic Intern. Nourvelle Serie I. Afrique del. Quest (ed. By Fabre, T.). Pergamon Oxford.

Robert, Lee Stahl (1973) Detection and Delineation of fault by surface resistivity measurements, Gas Hills Region Fremont and Natrona Counties, Wyo. Bureau of Mins Rpt of Investigation 7824 USGS.

Robert, Lee Stahl, (1974). Detection and Delineation of Faults by Surface Resistivity Measurements. Schwatzwalder Mine, Jefferson County, Colo. Bureau of Mines Rpt. No. 7975, USGS.

Sharma, P.V. (1987). Magnetic Method Applied to Mineral Exploration. Ore Geol. Rev., 2, 323 – 357.

Short, K.C. and Stauble, A.J. (1967). Outline of Geology of the Niger Delta. Bull. AAPG., Vol. 51, p. 761 – 779.

Simpson, A. (1954). The Nigerian Coal Fields, the Geology of Parts of Onitsha, Owerri and Benue Provinces Geol. Surv. Nig. Bull; 24.

Tattam, C.M. (1944). A Review of Nigerian Stratigraphy Rep. Geol. Surv. Nig. Bull 24, pp. 27 46.

Telford, W.M., Geldart, L.P., Sheriff, R.E., Keys, D.A. (1978) Applied Geophysics. Cambridge Univ. Press., Cambridge.

Umeji, A.C., (1980). Tertiary Planation Surfaces. On the Cuesta in Southeastern Nigeria, J. Min. Geol. 17 (2): 109 – 118.

Wordy, E. and Kogbe, C.A. (1983). Further Evidence of Marine Cenomanian, Lower Turonian and Maastrichtian in the Upper Benue Basin of Nigeria (West Africa). Cret. Res. Vol. 4., 95 – 99.

Zarboski, P.M.P. (1983). Campo-Maastrichtian Ammonites Correlation and Paleogeography in Nigeria Jour. Africa. Earth-Sciences. Earth-Science Vol. 4, pp. 59 – 63.